# Electrochemical Oxidation of 2-Pyrimidinethiols and Theoretical Study of Their Dimers, Disulfides, Sulfenyl Radicals, and Tautomers

**Fillmore Freeman***

*Department of Chemistry, University of California, Irvine, Irvine, California 92697-2025*

**Henry N. Po,* Thach S. Ho, and Ximeng Wang**

*Department of Chemistry and Biochemistry, California State University, Long Beach, Long Beach, California 90840*

*Received: August 14, 2007; In Final Form: November 19, 2007*

The relative energies and structures of 2-pyrimidinethiol (**1**), 4-methyl-2-pyrimidinethiol (**3**), 5-methyl-2-pyrimidinethiol (**5**), and 4,6-dimethylpyrimidinethiol (**7**), and their dimers, disulfides, sulfenyl radicals, and tautomers have been studied using restricted and unrestricted ab initio theory, density functional theory, complete basis set methods, coupled cluster theory, and quadratic configuration interaction calculations. The electrochemical oxidation of 2-pyrimidinethiol (**1**), 4-methyl-2-pyrimidinethiol (**3**), and 4,6-dimethylpyrimidinethiol (**7**) in ethanenitrile affords the respective disulfides in excellent yields. The less polar 2-pyrimidinethiol tautomers are predicted to be the dominant species in the gas phase. CBS-QB3, CBS-Q, CCD, CCSD(T), QCISD(T), and MP2 predict the energy difference ($E_{rel}$) between (**1**) and its tautomer (2-pyrimidinethione, **2**) to be in the narrow range from 7.23 to 7.87 kcal/mol. Similar trends are observed in the $E_{rel}$ values for the respective tautomers of 2-pyrimidinethiols (**3**), (**5**), and (**7**). The hybrid density functionals B3LYP, B3P86, B3PW91, and MPW1PW91 predict smaller values for $E_{rel}$ between the tautomers than any of the other models. Substitution of methyl groups at positions 4 and 6 of the pyrimidine ring lowers the energy difference between the respective tautomers while a methyl group at position 5 has little effect. The 2-pyrimidinethiol dimer (**13**) is predicted to be 5.52 and 4.12 kcal/mol, respectively, lower in energy than the isomeric 2-pyrimidinethione dimer (**14**) and heterodimer (**15**). The intramolecular four center transition states (**TS1**) for the tautomerization of 2-pyrimidinethiols (**1**, **3a**, **3b**, **5**, and **7**) in the gas phase have activation barriers of 34.84, 34.42, 34.02, 35.16, and 33.64 kcal/mol, respectively. Alternative lower energy pathways for tautomerism in the gas phase involve dimers and dimer transition states. Dimers and dimer transition states are also involved in the electrochemical oxidation of the 2-pyrimidinethiols. The APT, Mulliken (MPA), and NBO partial atomic charges are compared with the CHELPG and MKS charges that give the most consistent and similar results.

## Introduction

Sulfur centered radicals have received relatively little theoretical attention.[1,2] However, considerable effort has been devoted to the selection of antioxidants to prevent free radical induced oxidation in biological and chemical systems. Thiols are important antioxidants and are easily converted to their anions, radicals, and disulfides. Thiols, thiones, sulfenyl anions (thiolates, $RS^-$), sulfenyl radicals (thiyl, $RS^\bullet$), and disulfides also play important roles in diverse fields such as atmospheric chemistry, biological chemistry, environmental chemistry, industrial chemistry, organic synthesis, and medicine.[1] The disulfide linkage is important in biological functions in molecules such as cysteine, glutathione, and insulin. Pyrimidinethiols (−N═C−SH), pyrimidinethiones (−NH−C═S), and their derivatives have been used extensively in surface chemistry and in coordination chemistry because of the binding capabilities of nitrogen and sulfur to metals.[3−8] Pyrimidinethiols can coordinate with metals as a neutral species (−NH−C═S) or as a conjugate base (−N═C−$S^-$). Dimers, dimeric transition states, and tautomerism (eq 1) are probably involved in many of the properties and reactions described above for 2-pyrimidinethiols (2-mercaptopyrimidines).

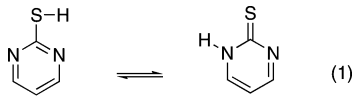


(1)

**1** **2**

The relative energies of tautomers and the mechanisms of the tautomerism of heterocyclic thiols and thiones also play significant roles in many areas of science. The respective tautomers of 2-pyrimidinethiol (**1**, **2**),[5,9] 4-methyl-2-pyrimidinethiol (**3a**, **3b**, **4a**, **4b**),[10] 5-methyl-2-pyrimidinethiol (**5**, **6**),[10] and 4,6-dimethyl-2-pyrimidinethiol (**7**, **8**, Figure 1)[9−11] are of special interest. There are only a few computational studies on the 2-pyrimidinethiol (**1**) ⇆ 2-pyrimidinethione (**2**) system: [UBPW91/6-31+G(d,p),[8] CNDO/2,[12] MNDO,[13] HF/3-21G(d),[14] MBPT(2)/6-31G(d),[14] and MP2.[15] Recently Freeman and Po[16] investigated the tautomerization mechanisms between (**1**) and (**2**) in the gas phase and in the aqueous phase using density functional theory (DFT). There are several theoretical reports on 4-methyl-2-pyrimidinethiol (**3**)[5,9] and only one computational report (B3PW91) on 4,6-dimethyl-2-pyrimidinethiol (**7**).[11a]

* Corresponding authors. F.F.: e-mail, ffreeman@uci.edu; tel, 949-824-6501; fax, 949-824-8571.

10.1021/jp076545y CCC: $40.75 
Published on Web 01/26/2008

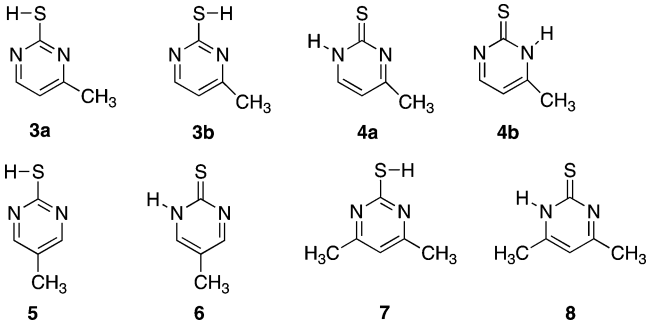


**Figure 1.** 2-Pyrimidinethiols (**3**, **5**, **7**) and their thione tautomers (**4**, **6**, **8**).

There is considerable discussion as to whether or not density functional methods are appropriate for calculating the relative energies of tautomeric cyclic thiols and thiones and the relative energies of organosulfur compounds.[5,15−23]

Computational studies on sulfur-containing compounds may show large basis set effects. We present an extensive systematic study on the choice of methods and basis sets for a wide range of structurally related species with important sulfur containing functional groups including thiols, thiones, disulfides, sulfenyl radicals, thiol dimers, thione dimers, and transition states in order to obtain accuracy at reasonable computational costs. We have calculated the relative energies of 2-pyrimidinethiols, 2-pyrimidinethiones, and their derivatives using restricted and unrestricted complete basis set methods (CBS-QB3, CBS-Q, CBS-4M), MP2, B3LYP, B3P86, B3PW91, MPW1PW91, CCD, CCSD(T), and QCISD(T) with the 6-31+G(d,p), 6-31++G(d,p), 6-311+G(d,p), 6-311++G(d,p), and cc-pVDZ basis sets in order to obtain reliable relative energies ($E_{rel}$) between tautomers, to study the mechanisms of tautomerization, and to explore the species involved in the electrochemical oxidation of 2-pyrimidinethiols. The 2-pyrimidinethiols (**1**, **3**, **5**, and **7**) are oxidized under a wide range of experimental conditions to the respective disulfides bis(2-pyrimidinyl) disulfide (**9**),[10,24−26] bis(4-methyl-2-pyrimidinyl) disulfide (**10**),[10,25−27] bis(5-methyl-2-pyrimidinyl) disulfide (**11**),[10] and bis(4,6-dimethyl-2-pyrimidinyl) disulfide (**12**, Figure 2).[9,10,25−28] We also report the electrochemical oxidation of 2-pyrimidinethiols (**1**), (**3**), and (**7**) to their respective disulfides (**9**), (**10**), and (**12**). The mechanism for the electrochemical oxidation of 2-pyrimidinethiols may involve sulfenyl anions and sulfenyl radicals,[1,29] and the electronic structures and relative energies of the relevant sulfenyl radicals that may be involved in the electrochemical processes have also been studied.

## Theoretical Methods

The calculations were carried out with the Spartan '04 Macintosh,[30] Spartan '02 Unix,[30] and Gaussian 03[31,32] computational programs. Equilibium geometry calculations were carried out with coupled cluster doubles (CCD), Moeller−Plesset second-order perturbation theory (MP2), and the hybrid density functionals B3LYP,[33−36] B3P86,[37] B3PW91,[33,34,36−38] and MPW1PW91[39] with the 6-31+G(d,p), 6-31++G(d,p), 6-311+G(d,p), 6-311++G(d,p),[40−44] and cc-pVDZ[45] basis sets. The 6-311+G(d,p) basis set is of triple-$\zeta$ quality for valence electrons, and basis sets with diffuse functions are useful for calculations of anions and structures with lone pairs.

No constraints were imposed on the structures during the equilibrium geometry calculations and during the transition state structure optimizations. Vibrational frequency analyses were carried out in order to assess the nature of the stationary points and to obtain zero point vibrational energies (ZPVEs). The characteristics of local minima were verified by establishing that the matrices of the energy second derivatives (Hessians) have no imaginary frequencies. The complete basis set (CBS) methods and the single point energy calculations on the optimized structures using coupled cluster singles, doubles, and triples models [CCSD, CCSD(T)] and quadratic configuration interaction models [QCISD, QCISD(T)] with the cc-pVDZ basis set were used to obtain the relative electronic energies ($E_{rel}$). The relative energy is the difference in calculated electronic energy without zero-point or other corrections. The relative enthalpy ($H(0)_{rel}$) is the difference in enthalpy at 0 K ($H(0)_{rel} = E_{rel}$ + ZPVE correction), which is also the free energy [$G(0)_{rel}$] at that temperature. $H(298)_{rel}$ and $G(298)_{rel}$ are the enthalpy and free energy differences corrected to 298.15 K. The zero point vibrational energies (ZPVE) for B3LYP, B3P86, B3PW91, and MP2 were scaled by 0.9804, 0.9759, 0.9772, and 0.9670, respectively, in the calculations of the relative thermodynamic parameters.[46,47] Total energies are in atomic units (au), and the other energies are in kcal/mol. Throughout this paper bond angles and torsion (dihedral) angles are in degrees, bond lengths are in angstroms (Å), dipole moments ($\mu$) are in debyes (D), atomic charges are in electrons, and entropies are in cal/mol-K.

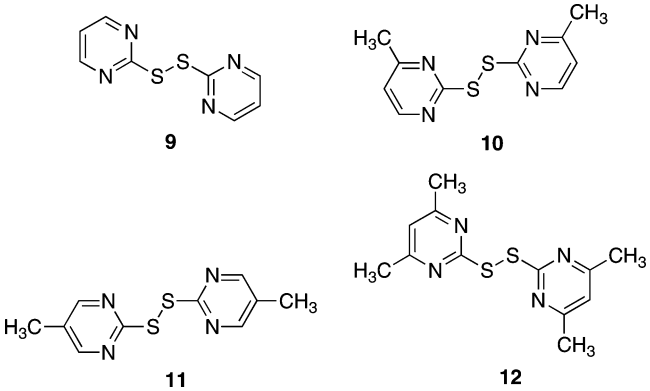


**Figure 2.** Bis(2-pyrimidinyl) disulfides (**9**), (**10**), (**11**), and (**12**).

## Experimental Section

**Reagents.** 2-Pyrimidinethiol (**1**), 4-methyl-2-pyrimidinethiol hydrochloride, and 4,6-dimethyl-2-pyrimidinethiol (**7**) were purchased from the Aldrich Chemical Co. 2-Pyrimidinethiols (**1**) and (**7**) were dissolved in 50% ethanol water solution at 60−70 °C, cooled, filtered, and dried in vacuum. 4-Methyl-2-pyrimidinethiol hydrochloride was dissolved in water at 50 °C, neutralized with 1 M NaOH, and the final pH of the solution adjusted to 10.5. The solution was cooled in a refrigerator overnight, and the precipitated 4-methyl-2-pyrimidinethiol (**3**) was separated by vacuum filtration and recrystallized from 50% aqueous ethanol. The physical properties of the 2-pyrimidinethiols (**1**, **3**, **7**) were in agreement with their respective literature values. The compounds were further characterized by mass spectrometry and ultraviolet−visible, FTIR, $^1$H NMR, and $^{13}$C NMR spectroscopy.

Tetraethylammonium perchlorate (TEAP) was purchased from G. F. Smith Chemical and was recrystallized from a 1:1 (v:v) ethanol/water solution. Glass distilled high purity ethanenitrile ($CH_3CN$) was purchased from Burdick and Jackson and used as received without further purification. All other solvents used in the recrystallization and extraction procedures were of reagent grade.

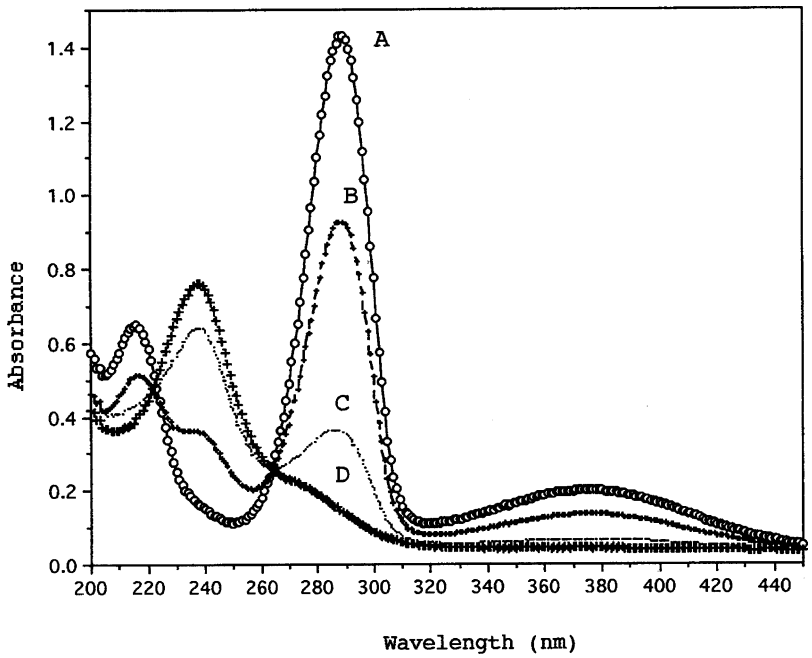


**Figure 3.** Spectra of the appearance of disulfide (**9**) and the disappearance of 2-pyrimidinethione (**2**) during electrosynthesis. Curve **A**, time 0; **B**, 3 min; **C**, 13 min; and **D**, 41 min.

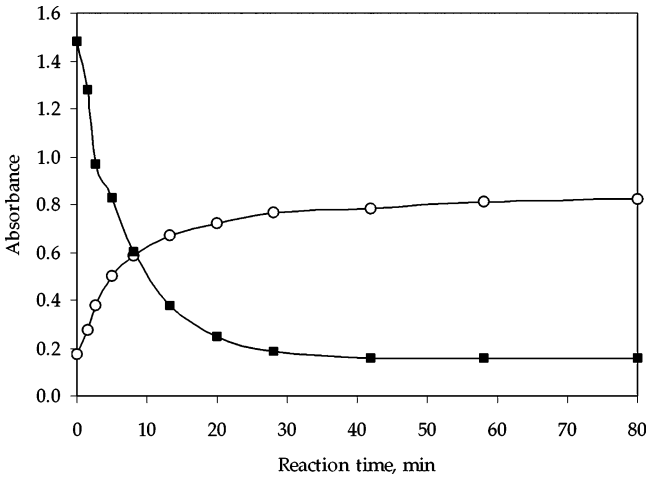


**Figure 4.** Absorbance changes during the electrochemical oxidation of 2-pyrimidinethiol (**1**/**2** at 289 nm, dark squares) to the disulfide (**9** at 238 nm, open circles) as a function of time.

Elemental analyses were performed by Atlantic Microlab, Inc. and NMR measurements ($\delta$ in ppm) were done in DMSO-$d_6$ (TMS reference).

**Cyclic Voltammetry.** Cyclic voltammetry (CV) scans were performed on (**1**, **3**, **7**) in ethanenitrile to determine their oxidation potential for controlled-potential synthesis. A Princeton Applied Research electrochemical system consisting of a potentiostat/galvanostat, a Universal Programmer, and a digital coulometer was used. The CV cell is a three-electrode cell that consists of a Pt disk working electrode, a Ag/AgCl reference electrode, and an auxiliary Pt foil electrode placed inside a fritted disk glass tube. The electrolytic solution used was 0.1 M TEAP in ethanenitrile that was degassed with purified dinitrogen which was passed through an Oxiclear trace dioxygen remover and a bubbler filled with the solvent. An initial CV scan of the electrolyte solution was taken to ensure that no electroactive impurities were present. A 2-pyrimidinethiol (**1**, **3**, or **7**) concentration of $1.00 \times 10^{-3}$ M (e.g., 6.7 mg or $6 \times 10^{-5}$ mol (**1**) in 60 mL) in ethanenitrile was prepared and scanned at a rate of 100, 200, and 500 mV/s. The CV of (**1**) showed an irreversible anodic peak at $Ep_a = 0.62$ V and on reverse scan a cathodic peak at $Ep_c = -0.32$ V. All potentials are given in reference to the Ag/AgCl electrode. The cathodic peak was not present when the scan was initiated from the positive to the negative potential region. This means that the cathodic peak observed during the reverse scan was due to the reduction of the disulfide (**9**) back to 2-pyrimidinethiol (**1**). The respective anodic potentials for thiols (**3**) and (**7**) are 0.79 and 0.87 V and their cathodic potentials are $-0.33$ and $-0.43$ V, respectively. The $Ep_a$ was found to increase with methyl substituents on the pyrimidine ring (**1**, **3**, **7**), from $+0.62$ to $+0.87$ V. The anodic potential tends to become more positive in subsequent scans, which suggests the adsorption of sulfenyl anion ($R-S^-$) on the metal surface forming Pt$-$S bonds and polymers of Pt$(-SR)_n$.[10]

**Electrochemical Synthesis of Disulfides.** The electrosyntheses of disulfides (**9**, **10**, **12**) were carried out at potentials slightly higher than the $Ep_a$ recorded in the cyclic voltammetry studies. This was done to ensure complete oxidation of the thiol. An electro-cell consists of cylindrical Pt mesh electrode of 4 cm (d) $\times$ 3 cm (h), a smaller auxiliary cylindrical Pt mesh electrode of 1 cm (d) $\times$ 2.5 cm (h), and a Ag/AgCl reference electrode. During the experiment, the electro-cell was wrapped with aluminum foil to exclude light. A typical $5 \times 10^{-3}$ M solution of 2-pyrimidinethiol (e.g., **1**, 39.3 mg or $3.5 \times 10^{-4}$ mol in 70 mL of 0.1 M TEAP/ $CH_3CN$) was prepared and degassed with purified dinitrogen for 15 min to remove dissolved dioxygen. During the electrosynthesis, the solution was kept under dinitrogen and stirred continuously. Aliquot samples of 100 $\mu$L (microliter) were removed every 5 min and diluted with 5 mL of ethanenitrile for spectral and thin layer chromatography (TLC) analysis. The TLC separation of the two compounds was done on an alumina-coated plate using 1:1 (vol: vol) $CH_3OH/CH_2Cl_2$ mixture as the eluting solvent. Figure 3 shows the UV$-$vis spectral changes as a function of time at 289 nm due to the disappearance of 2-pyrimidinethione (**1**, **2**) and the increase absorbance of the disulfide (**9**) at 238 nm. Figure 4 shows the formation curve of (**9**) and the disappearance curve of (**1**, **2**) reaching plateaus after about 45 min of

**TABLE 1: Relative Energy for 2-Pyrimidinethiol (1) and 2-Pyrimidinethione (2)**

| level of theory | $E_{rel}$[a] | level of theory | $E_{rel}$[a] |
|---|---|---|---|
| CBS-QB3 | 7.37 | B3P86/6-311+G(d,p) | 3.28 |
| CBS-Q | 7.23 | B3P86/6-311++G(d,p) | 3.28 |
| CCD/cc-pVDZ | 7.70 | B3PW91/6-31+G(d,p) | 3.05 |
| CCSD/cc-pVDZ[b] | 8.00 | B3PW91/6-311+G(d,p) | 3.42 |
| CCSD/cc-pVDZ(T)[b] | 7.87 | B3PW91/6-311++G(d,p) | 3.41 |
| QCISD/cc-pVDZ[b] | 7.43 | MP2/6-31+G(d,p) | 7.47 |
| QCISD/cc-pVDZ(T)[b] | 7.68 | MP2/6-31++G(d,p) | 7.48 |
| B3LYP/6-311+G(d,p) | 3.60 | MP2/6-311+G(d,p) | 8.84 |
| B3LYP/6-311++G(d,p) | 3.60 | | |

[a] $E_{rel} = E$(thione) − $E$(thiol). [b] CCD/cc-pVDZ optimized structure.

**TABLE 2: Relative Energies for 2-Pyrimidinethiols (3, 5, 7) and 2-Pyrimidinethiones (4, 6, 8)**

| | $E_{rel}$[a] | | | |
|---|---|---|---|---|
| level of theory | **3a**, **4a** | **3b**, **4b** | **5**, **6** | **7**, **8** |
| CBS-QB3 | 6.70 | 6.92 | 7.58 | |
| CBS-Q | 6.40 | 6.54 | 7.23 | 5.23 |
| CCD/cc-pVDZ | 6.66 | 6.83 | 9.11 | |
| CCSD/cc-pVDZ[b] | 7.18 | 7.35 | 7.78 | |
| CCSD/cc-pVDZ(T)[b] | 7.18 | 7.30 | 7.91 | |
| QCISD/cc-pVDZ[b] | 6.64 | 6.83 | 7.40 | |
| QCISD/cc-pVDZ(T)[b] | 6.99 | 7.12 | 7.71 | |
| B3LYP/6-31+G(d,p) | 2.80 | 2.91 | 3.53 | 2.41 |
| CCSD/cc-pVDZ[c] | 7.17 | 7.82 | 8.06 | 6.71 |
| QCISD/cc-pVDZ[c] | 6.71 | 6.83 | 7.46 | 6.16 |
| B3LYP/6-31++G(d,p) | 2.79 | 2.90 | | |
| CCSD/cc-pVDZ[d] | 7.29 | 7.46 | | |
| QCISD/cc-pVDZ[d] | 6.71 | 6.89 | | |
| B3P86/6-31+G(d,p) | 2.32 | 2.45 | | 1.91 |
| B3PW91/6-31+G(d,p) | 2.43 | 2.55 | 3.53 | 2.01 |
| CCSD/cc-pVDZ[e] | 7.28 | 7.46 | 8.09 | 6.72 |
| CCSD(T)/cc-pVDZ[e] | | | | 6.63 |
| QCISD/cc-pVDZ[e] | 6.72 | 6.91 | 7.48 | 6.19 |
| QCISD(T)/cc-pVDZ[e] | | | | 6.44 |
| B3PW91/6-31++G(d,p) | 2.42 | 2.53 | | |
| CCSD/cc-pVDZ[f] | 7.28 | 7.46 | | |
| QCISD/cc-pVDZ[f] | 6.72 | 6.91 | | |
| MP2/6-31+G(d,p) | 6.84 | 7.13 | 7.83 | 6.50 |

[a] $E_{rel} = E$(thione) − $E$(thiol). [b] CCD/cc-pVDZ optimized structure. [c] B3LYP/6-31+G(d,p) optimized structure. [d] B3LYP/6-31++G(d,p) optimized structure. [e] B3PW91/6-31+G(d,p) optimized structure. [f] B3PW91/6-31++G(d,p) optimized structure.

controlled-potential. At this point, the TLC showed only one spot indicating only the disulfide (**9**) was present.

The solution was transferred to a round-bottom flask and the solvent removed under vacuum at 60 °C in a rotary flash evaporator. The solid was dissolved in water, pH adjusted to 7 with an appropriate amount of 1 M HCl or 1 M NaOH, and extracted with 3 × 20 mL of diethyl ether. The organic layer was removed and dried over anhydrous $Na_2SO_4$. The $Na_2SO_4$ was removed by filtration and the solvent was removed from the filtrate under vacuum at room temperature to give disulfide (**9**) as a light yellow solid. The solid was dried in vacuum and crystallized from methanol. The disulfide (**9**) was purified further from a 1:1 (vol:vol) acetone/petroleum ether solution in a container wrapped with aluminum foil to exclude light. It was dissolved in the mixed solvent at about 45 °C. Activated charcoal powder was added, and the mixture was stirred for 1 h and filtered. The filtrate was allowed to stand overnight at room temperature and filtered, and the solid was washed with a cold solution of acetone/petroleum ether and dried under vacuum. The overall yields of disulfides (**9**), (**10**), and (**12**) were over 90%.

**TABLE 3: Comparison of MP2/6-31+G(d,p) Partial Atomic Charges for 2-Pyrimidinethiol (1), 2-Pyrimidinethione (2), and the 2-Thiopyrimidinyl Radical (19)**

| atom | CHELG | MKS | NBO | APT | MPA |
|---|---|---|---|---|---|
| **1** | | | | | |
| N1 | −0.837 | −0.786 | −0.591 | −0.529 | −0.252 |
| C2 | +0.856 | +0.715 | +0.342 | +0.664 | −0.036 |
| N3 | −0.720 | −0.661 | −0.579 | −0.511 | −0.237 |
| C4 | +0.580 | +0.543 | +0.141 | +0.304 | +0.035 |
| C5 | −0.660 | −0.748 | −0.403 | −0.194 | −0.216 |
| C6 | +0.646 | +0.627 | +0.139 | +0.293 | +0.042 |
| S7 | −0.309 | −0.269 | +0.077 | −0.205 | +0.062 |
| S-H | +0.208 | +0.219 | +0.145 | +0.058 | +0.062 |
| **2** | | | | | |
| N1-H | +0.254 | +0.268 | +0.477 | +0.218 | +0.385 |
| N1 | −0.447 | −0.392 | −0.682 | −0.507 | −0.446 |
| C2 | +0.722 | +0.546 | +0.325 | +0.935 | +0.194 |
| N3 | −0.782 | −0.733 | −0.571 | −0.645 | −0.222 |
| C4 | +0.759 | +0.763 | +0.192 | +0.588 | +0.078 |
| C5 | −0.654 | −0.794 | −0.440 | −0.371 | −0.241 |
| C6 | +0.368 | +0.371 | +0.164 | +0.238 | +0.073 |
| S7 | −0.519 | −0.454 | −0.218 | −0.626 | −0.405 |
| **19** | | | | | |
| N1 | −0.719 | −0.685 | −0.583 | −0.525 | −0.254 |
| C2 | +0.796 | +0.724 | +0.288 | +0.697 | −0.012 |
| N3 | −0.719 | −0.685 | −0.583 | −0.525 | −0.254 |
| C4 | +0.552 | +0.526 | +0.141 | +0.305 | +0.031 |
| C5 | −0.602 | −0.657 | −0.402 | −0.196 | −0.217 |
| C6 | +0.552 | +0.526 | +0.141 | +0.305 | +0.031 |
| S7 | −0.111 | −0.087 | +0.267 | −0.185 | +0.129 |

A plot similar to Figure 4 that was obtained during the electrochemical oxidation of 4,6-dimethyl-2-pyrimidinethiol (**7**/**8**) to its disulfide (**12**) is shown in Figure SI-1 in the Supporting Information. The physical properties, elemental analysis, and spectral data for bis(2-pyrimidinyl) disulfide (**9**), bis(4-methyl-2-pyrimidinyl) disulfide (**10**), and bis(4,6-dimethyl-2-pyrimidinyl) disulfide (**12**) are given in the Supporting Information.

## Results and Discussion

**Levels of Theory and Relative Energies**. Owing to the possibility of basis set effects, it was necessary to establish reliable levels of theory for the computational study of the organosulfur structures and the relative energies of the tautomers of 2-pyrimidinethiols.[5,15−23] The coupled cluster theory of Bartlett and co-workers,[48−50] including single, double, and triple excitations (CCD, CCSD, CCSD(T)), has been found to be one of the best methods for calculating energy differences, and it is excellent for estimating electron correlation energy. Quadratic configuration interaction (QCISD) is closely related to coupled cluster theory and is also excellent for estimating electron correlation energy.[51,52] The highly accurate complete basis set (CBS) models were developed by Petersson and co-workers[53,54] with the idea that a major source of error in quantum mechanical calculations arises from basis set truncation. The CBS methods are among the most accurate multicomponent quantum mechanical methods, including the G-series developed by Pople and co-workers[55,56] and the W-series developed by Martin and co-workers,[57,58] that are capable of producing accurate (±1 kcal/mol) thermochemical data.

CBS-QB3 is the most accurate of the CBS models and includes the minimum population localization method. It is a five-step procedure that starts with B3LYP/CBSB7 geometry and frequency calculations, followed by CCSD(T)/6-31+G(d,p), MP4SDQ/CBSB4, and MP2/CBSB3 single point energy calculations, and a CBS extrapolation.[53,54] The CBS-Q model is similar to CBS-QB3 and starts with a geometry optimization at the MP2/6-31G(d′) level of theory, and the zero point energy

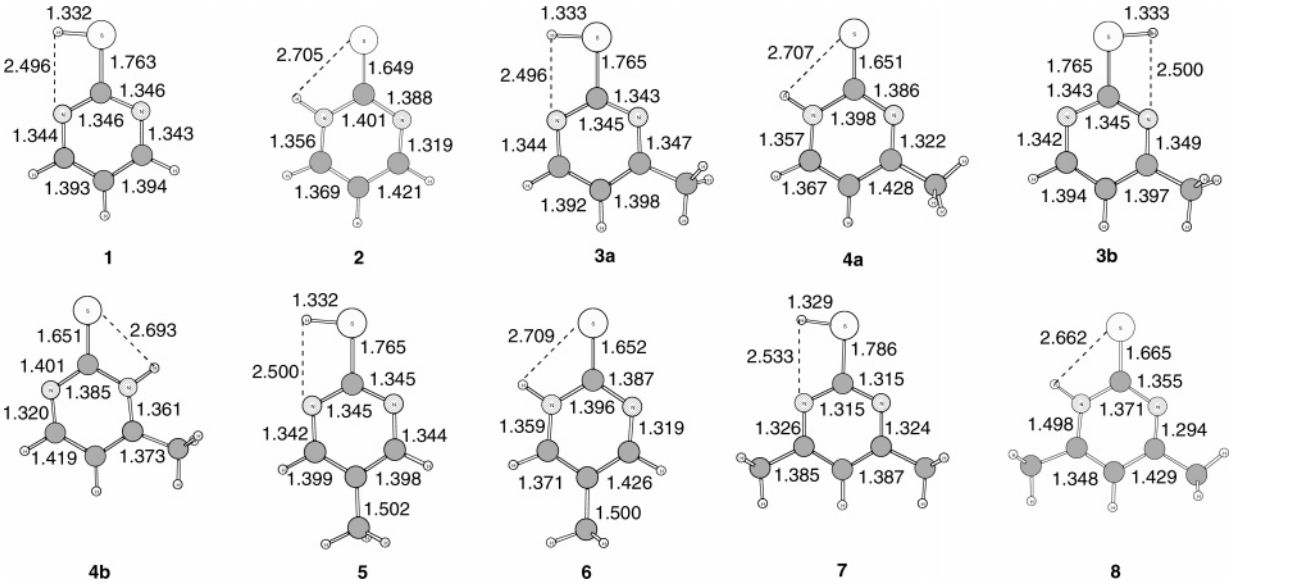


**Figure 5.** MP2/6-31+G(d,p) optimized structures of 2-pyrimidinethiol, 4-methyl-2-pyrimidinethiol, 5-methyl-2-pyrimidinethiol, 4,6-dimethyl-2-pyrimidinethiol, and their tautomers.

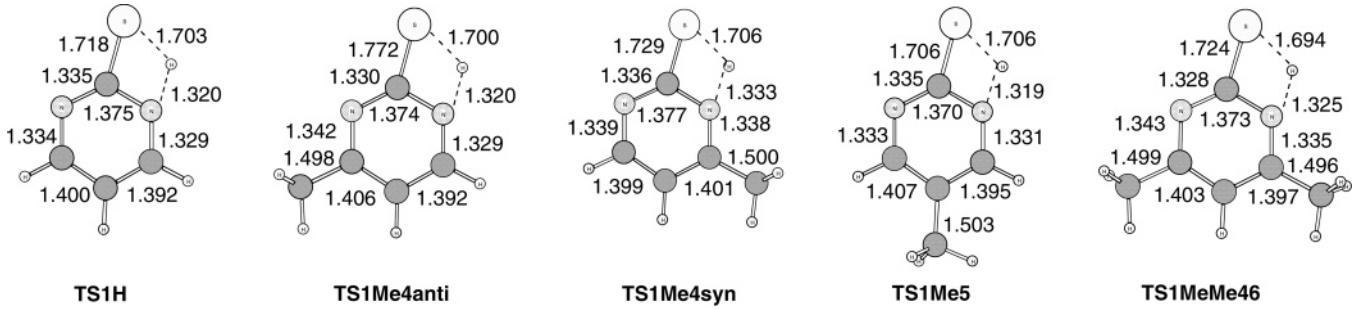


**Figure 6.** B3PW91/6-31+G(d,p) optimized transition states for the tautomerization of 2-pyrimidinethiols.

is calculated at the HF/6-31G(d) level. A large basis set SCF calculation [(HF/6-311+G(3d2f,2df,2p)] is used as a base energy, and a MP2/6-311+G(3d2f,2df,2p) calculation with a CBS extrapolation is used to correct the energy through second order. Two additional calculations are used to approximate higher order contributions: MP4(DQ)/6-31+G(d(f)d,f) with extra polarization functions on chlorine, phosphorus, and sulfur to approximate the higher order correlation effects and QCISD-(T)/6-31G(d′) for still higher order effects. CBS-Q has an empirical correction for spin contamination and a size-consistent higher order size correction. CBS-4M is less accurate and less computationally expensive than either CBS-QB3 or CBS-Q. It also includes the minimum population localization method and begins with a HF/3-21G(d) geometry optimization followed by a frequency calculation. It then uses a large basis set SCF calculation [HF/6-311+G(3d2f,2df,p)] as a base energy, and an MP2/6-31+G(d) calculation with a CBS extrapolation to correct the energy through second order. A MP4(DQ)/6-31+G(d,p) calculation is used to approximate higher order contributions before the CBS extrapolation.

Tables 1 and 2 show the effects of different levels of theory on the values of the relative energy ($E_{rel}$) between isomers and tautomers of the 2-pyrimidinethiols (**1**), (**3**), (**5**), and (**7**). The less polar pyrimidinethiol tautomer is the dominant species in the gas phase, and 4-methyl-2-pyrimidinethiol (**3a**) is 2.84 kcal/mol lower in energy than 5-methyl-2-pyrimidinethiol (**5**). CBS-QB3, CBS-Q, CCSD, CCD, QCISD, and MP2 predict the energy difference ($E_{rel}$) between (**1**) and its tautomer (2-pyrimidinethione, **2**) to be in the narrow range of 7.23−7.87 kcal/mol. Similar trends are predicted for the $E_{rel}$ values of the tautomers of 2-pyrimidinethiols (**3**), (**5**), and (**7**). CCSD predicts larger energy differences ($E_{rel}$) between tautomers than QCISD and QCISD/cc-pVDZ predicts $E_{rel}$ values closer to CBS-QB3 and CBS-Q than QCISD(T)/cc-pVDZ. The 6-31+G(d,p) and 6-31++G(d,p) or the 6-311+G(d,p) and 6-311++G(d,p) basis sets predict the same value of $E_{rel}$ (Tables 1 and 2). However, although the differences are small, MP2/6-31+G(d,p) predicts values of $E_{rel}$ closer to CBS-QB3, CBS-Q, and CCD/cc-pVDZ than MP2/6-311+G(d,p). The hybrid density functionals B3LYP, B3P86, B3PW91, and MPW1PW91 predict smaller values for $E_{rel}$ between tautomers than any of the other models used in this study. This is true irrespective of the basis set used and the inclusion of diffuse functions.[59] It is also seen in Tables 1 and 2 that increasing the number of methyl groups at positions 4 and 6 on the pyrimidine ring of (**1**) lowers the energy difference ($E_{rel}$) between the respective tautomers while a methyl group at position 5 has little effect.

**Structures of Tautomers.** The sulfanyl hydrogen (S−H) in 4-methyl-2-pyrimidinethiol (**3**) can exist in either the anti (**3a**) or syn (**3b**) conformation relative to the methyl group. Similarly, the N−H bond in (**4**) can exist in either the anti (4-methyl-2(1*H*)-pyrimidinethione, **4a**) or syn (4-methyl-2(3*H*)-pyrimidinethione **4b**) conformation relative to the methyl group. There are small energy differences among the tautomers of 4-methyl-2-pyrimidinethiol (**3a**, **3b**, **4a**, **4b**), and CBS-QB3 predicts the energy difference between (**3a**) and (**3b**) and between (**4a**) and

**TABLE 4: Relative Energies for 2-Pyrimidinethiols (1, 3, 5, 7) and Their Transition States (TS1)[a]**

| | TS1 | | | | |
|---|---|---|---|---|---|
| level of theory | **H** | **Me4a** | **Me4s** | **Me5** | **Me46** |
| CBS-4M | 31.93 | 31.45 | | | |
| B3LYP[b] | 30.94 | | | 31.34 | 29.94 |
| B3LYP[c] | 31.18 | | | | |
| B3PW91[b] | 29.06 | 28.64 | 28.42 | 29.46 | 28.03 |
| B3PW91[c] | 29.03 | | | | |
| MP2[b] | 34.61 | 34.56 | 34.15 | 35.16 | |
| MP2[c] | 34.14 | | | | |
| CCSD[d,e] | 35.30 | 34.85 | 34.46 | 35.60 | 34.05 |
| CCSD(T)[d,e] | 32.77 | 32.45 | 32.04 | 33.09 | 31.72 |
| QCISD[d,e] | 34.84 | 34.42 | 34.02 | 35.16 | 33.64 |
| QCISD(T)[d,e] | 32.55 | 32.23 | 31.82 | 32.87 | 31.51 |

[a] $E_{rel} = E(\mathbf{TS1}) - E(\text{thiol})$. [b] 6-31+G(d,p) basis set. [c] 6-311+G(d,p) basis set. [d] cc-pVDZ basis set. [e] B3LYP/6-31+G(d,p) or B3PW91/6-31+G(d,p) optimized structure.

(**4b**) to be 0.05 and 0.28 kcal/mol, respectively. Unlike thiol (**3**), one ground state structure of 2-pyrimidinethiol (**1**), of 5-methyl-2-pyrimidinethiol (**5**), and of 4,6-dimethyl-2-pyrimidinethiol (**7**) were considered. Similarly, one ground state structure of 2-pyrimidinethione (**2**), 5-methyl-2-pyrimidinethione (**6**), and 4,6-dimethyl-2-pyrimidinethione (**8**) were investigated.

C−S bond lengths in simple dialkyl sulfides and diaryl sulfides have the mean average distance of 1.82 Å and 1.75 Å, respectively.[60] Resonance between the 2p orbitals of the ring carbon and 3p orbitals of sulfur contributes to the shorter bonds in the diaryl disulfides. Selected geometrical parameters for the 2-pyrimidinethiols (**1**, **3**, **5**, **7**) and 2-pyrimidinethiones (**2**, **4**, **6**, **8**) are shown in Figure 5. Several levels of theory predict the C−S bond lengths in the 2-pyrimidinethiols (**1**, **3a**, **3b**, **5**, **7**) to be close to 1.765 Å and their S−H bond lengths to be 1.333 Å. The predicted thiocarbonyl (C═S) bond lengths in the 2-pyrimidinethiones (**2**, **4**, **6**, **8**) are close to 1.665 Å, which is consistent with the double bond character. Unlike the 2-pyrimidinethiones, the bond lengths in the heteroaromatic rings of the 2-pyrimidinethiols are consistent with their aromatic character.[61] The N1−C2−N3 bond angles in the 2-pyrimidinethiols are near 127°, and these angles in the 2-pyrimidinethiones are near 116°. The N1−C2−S7 bond angles in the 2-pyrimidinethiols are near 115°, and these angles in the 2-pyrimidinethiones are near 120°.

Selected intramolecular nonbonded N−H−S distances in the 2-pyrimidinethiols and the intramolecular nonbonded S−H−N distances in the 2-pyrimidinethiones are shown in Figure 5.[62] Attractive electrostatic interactions between the nitrogen atom and the sulfanyl hydrogen in the thiols and between the N−H bond hydrogen and sulfur atom in the thiones are possible. These interactions are reasonable since the optimized N−H−S separation is smaller than the sum of the van der Waals radii for hydrogen (1.20 Å) and nitrogen (1.55 Å) in the 2-pyrimidinethiols and the hydrogen nonbonded sulfur distance is less than the sum of the van der Waals radii for hydrogen and sulfur (1.80 Å) in the 2-pyrimidinethiones. In 2-pyridinethiol the intramolecular N−H−S interaction is worth approximately 1.4 kcal/mol.[17]

## Partial Atomic Charges of Disulfides, Thiols, and Thiones

Although partial atomic charges on atoms can be neither measured nor obtained unambiguously from quantum chemical calculations, they are an integral part of all aspects of science including mechanisms and structures in chemistry.[63−70] The distribution of atomic charges is of particular interest in nonbonding interactions, hydrogen bonding, and dimer formation. Several schemes are widely employed to calculate partial atomic charges, but there is no one scheme that is best for all systems. Each method offers distinct advantages, each scheme suffers from disadvantages, and the calculated atomic charges are dependent on the level of theory used. It is known that the Mulliken population analysis (MPA)[65] may fail when extended basis sets and diffuse functions are used and that NBO (natural bond orbital analysis, NPA, natural population analysis)[66] may lead to exaggerated C−H bond dipoles. The MP2/6-31+G(d,p) partial atomic charges of 2-pyrimidinethiols (**1**, **3**, **5**, **7**), and 2-pyrimidinethiones (**2**, **4**, **6**, **8**) using NBO, electrostatic potential-derived charges in the CHELPG scheme,[67] electrostatic potential-derived charges in the Merz−Kollman−Singh scheme (MKS),[68] and an approach that makes use of atomic polar tensors (GAPT or APT)[69,70] are shown in Table 3 and in Tables SI-1, SI-2, SI-3, and SI-4 in the Supporting Information. A comparison of MP2/6-31+G(d,p) and B3PW91/6-31+G(d,p) partial atomic charges for 2-pyrimidinethiol (**1**) and 2-pyrimidinethione (**2**) is available with Table 3 and Table SI-5 in the Supporting Information.

Among the five population analysis schemes, the Mulliken calculations deviate the most from the trends generated by the other four methods (Tables 3, SI-1, SI-2 SI-3, SI-4). The partial atomic charges calculated by APT, CHELPG, and MKS are similar, and CHELPG and MKS give the most consistent results. Owing in part to greater electronegativity, the nitrogen atoms have the most negative charges with CHELPG and MKS calculating very negative values. It is seen in the tables that the partial atomic charges on the nitrogens are unequal, that C5 has a partial negative charge, and that the thiocarbonyl sulfur has partial negative charge more negative than the sulfanyl sulfur in all tautomers (**1**−**8**). Although all schemes are in agreement on the nitrogen atoms, they do not agree on the partial atomic charges on sulfur and the methyl group carbons. For 2-pyrimidinethiols (**1**, **3**, **5**, **7**), only NBO predicts a partial positive charge on sulfur and for tautomers (**3**), (**4**), (**5**), (**7**) and (**8**) only APT predicts partial positive charges on the methyl carbons. For the thiones (**2**, **4**, **6**, **8**) all schemes predict partial negative charges on sulfur and on the methyl carbons.

The B3PW91/6-31+G(d,p) calculated APT, CHELPG, MKS, and NBO partial atomic charges on the sulfur atoms in (**1**) and (**2**) (Table SI-5 in the Supporting Information) and in the disulfides (**9**, **10**, **12**) are equal and negative (Table SI-6 in the Supporting Information). For example, a comparison of the two levels of theory using 2-pyrimidinethione (**2**) shows that the smallest differences are with CHELPG, MKS, and NBO. Only Mulliken predicts positive partial charges on the sulfur atoms. The charges on the respective atoms are equal except for nitrogen where one atom has a slightly more negative charge than the other.

## Spectral Data of Disulfides, Sulfenyl Radicals, Thiols, and Thiones

The calculated vibrational spectra of the 2-pyrimidinethiols (**1**, **3**, **5**, **7**) show the S−H stretching frequency in the 2600−2800 $cm^{-1}$ region. These predictions are in agreement with the experimental values reported for organosulfur compounds containing the sulfanyl group.[8,71] Although the S−H stretching frequency has a relatively low intensity, it is useful for detecting the sulfanyl group since few other groups show absorption in this region. The involvement of intramolecular and intermolecular hydrogen bonds influences the absence, presence, and intensity of the S−H stretching frequency. The weak and

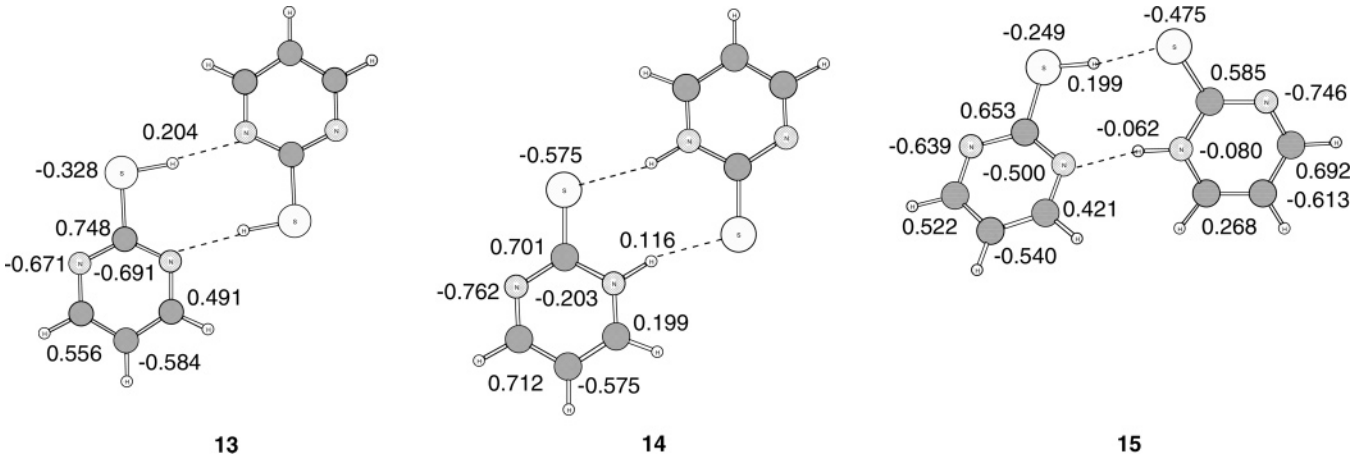


13 14 15

**Figure 7.** B3PW91/6-31+G(d,p) optimized structures and CHELPG charges for the 2-pyrimidinethiol dimer (**13**), 2-pyrimidinethione dimer (**14**), and thiol/thione heterodimer (**15**).

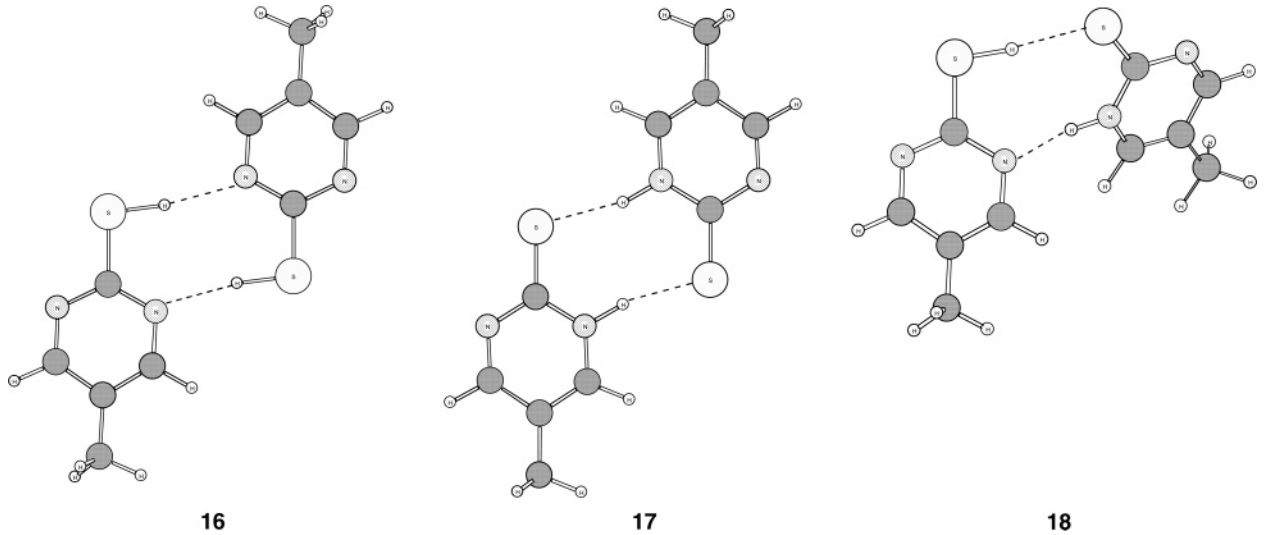

16 17 18

**Figure 8.** B3PW91/6-31+G(d,p) optimized structures for the 5-methyl-2-pyrimidinethiol dimer (**16**), 5-methyl-2-pyrimidinethione dimer (**17**), and thiol/thione heterodimer dimer (**18**).

**TABLE 5: MP2/6-31+G(d,p) Partial Atomic Charges for Transition States TS1H and TS1Me5**

| | TS1H | | | | | TS1Me5 | | | | |
|---|---|---|---|---|---|---|---|---|---|---|
| atom | CHELPG | MKS | NBO | APT | Mulliken | CHELPG | MKS | NBO | APT | Mulliken |
| N1 | −0.499 | −0.447 | −0.717 | −0.612 | −0.249 | −0.372 | −0.365 | −0.574 | −0.620 | −0.215 |
| C2 | +0.732 | +0.580 | +0.363 | +0.686 | +0.078 | +0.618 | +0.563 | +0.239 | +0.684 | +0.148 |
| N3 | −0.747 | −0.689 | −0.572 | −0.559 | −0.224 | −0.627 | −0.625 | −0.469 | −0.552 | −0.213 |
| C4 | +0.657 | +0.650 | +0.183 | +0.421 | +0.098 | +0.398 | +0.416 | +0.087 | +0.365 | +0.012 |
| C5 | −0.625 | −0.695 | −0.437 | −0.310 | −0.262 | −0.138 | −0.068 | −0.152 | −0.169 | +0.266 |
| C6 | +0.444 | +0.416 | +0.194 | +0.346 | +0.051 | +0.188 | +0.182 | +0.089 | +0.289 | −0.063 |
| S7 | −0.447 | −0.401 | −0.191 | −0.617 | −0.342 | −0.381 | −0.366 | −0.112 | −0.638 | −0.343 |
| S-H | +0.195 | +0.206 | +0.423 | +0.470 | +0.274 | +0.151 | +0.342 | +0.422 | +0.484 | +0.271 |
| C8 | | | | | | −0.170 | −0.510 | −0.712 | +0.106 | −0.671 |

variable C−S stretching vibration is seen in the region of 400 and 500 $cm^{-1}$. The calculated vibrational spectra of the 2-pyrimidinethiones (**2**, **4**, **6**, **8**) are consistent with experimental spectra of thiocarbonyl compounds showing the C═S absorption in the 1000−1250 $cm^{-1}$ region. Bands are also observed in the 700−1565 $cm^{-1}$ region owing to vibrations between C−N and C═S stretching. The S−S stretching vibration in the disulfides is very weak and falls between 400 and 600 $cm^{-1}$. Disulfide (**9**) shows a weak band at 552 $cm^{-1}$ due to the S−S bond. A similar S−S stretching frequency at 544 $cm^{-1}$ is observed for disulfide (**10**) and for disulfide (**12**). The predicted vibrational frequencies for the sulfenyl radicals are similar to those of the 2-pyrimidinethiols and 2-pyrimidinethiones but do not show the S−H stretching frequency in the 2600−2800 $cm^{-1}$ region and the N−H stretching frequency in the 3400 $cm^{-1}$ region.

In ethanenitrile, the ultraviolet spectrum of 2-pyrimidinethione (**2**) shows absorptions at 377 nm, ($\log \epsilon = 3.29$), 289 nm ($\log \epsilon = 4.22$), and 216 nm ($\log \epsilon = 3.82$). In water, the absorptions are at 373 nm ($\log \epsilon = 3.29$), 291 nm ($\log \epsilon = 3.29$), and 214 nm ($\log \epsilon = 3.29$).[9] The absorption maxima ($\lambda_{max}$) in ethanenitrile for the 2-pyrimidinethiones (**4**) and (**8**) are both at 288 nm with $\log \epsilon = 4.22$ and $\log \epsilon = 4.25$, respectively. The ultraviolet−visible spectra of the 2-pyrimidinethiols/2-pyrimidinethiones and the corresponding disulfides are very different. The absorption spectra of the disulfides (**9**, **10**, and **12**) are similar with each showing an intense peak at 238 nm ($\log \epsilon =$

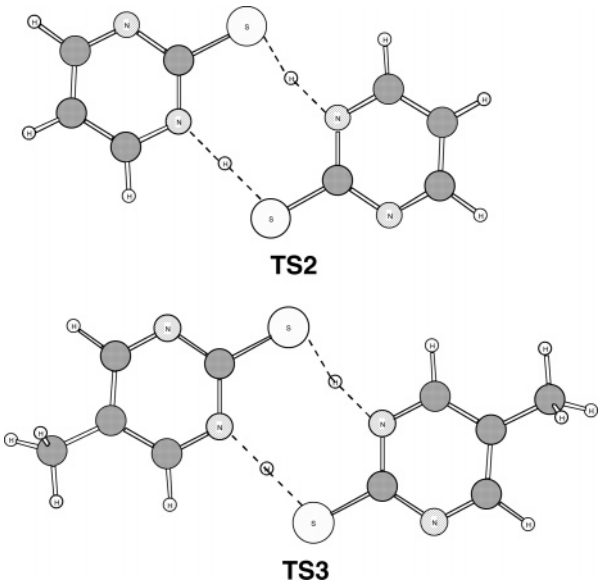


**Figure 9.** B3PW91/6-31+G(d,p) optimized structures for transition states **TS2** and **TS3**.

4.26), 239 (4.24) and 240 (4.23), respectively, with a weak shoulder absorption at about 275 nm (log $\epsilon$ about 3.78).

### Tautomerization Mechanisms

The gas phase tautomerization mechanism of 2-pyrimidinethiols may involve strained intramolecular four centered transition state structures (**TS1**, Figure 6, Table 4) in which the proton transfers from sulfur to the pyrimidine ring nitrogen or dimer transition states. Each of the five transition state structures (**TS1**) has one imaginary frequency and shows the four center pattern involving the C−S−H−N atoms. The N1−C2−S7 bond angle decreases as the 2-pyrimidinethiol goes to the transition state (**TS1**). Intrinsic reaction coordinate (IRC) calculations show that these transition states connected the respective 2-pyrimidinethiol and 2-pyrimidinethione.[72] None of the transition states (**TS1**) shows S−H stretching in the 2600−2800 $cm^{-1}$ region indicating that the S−H bond is essentially broken since it has increased in length from 1.333 Å to 1.703 Å. QCISD/cc-pVDZ//B3PW91/6-31+G(d,p) predicts these barriers to tautomerization to be 34.84, 34.42, 34.02, 35.16 and 33.64 kcal/mol, respectively, for (**1**, **2**), (**3a**, **4a**), (**3b**, **4b**), (**5**, **6**), and (**7**, **8**).[16] Similar barriers were calculated at the MP2/6-31+G(d,p) level of theory. The energy difference ($E_{rel}$) between 2-pyridinethiol and it intramolecular four center transition state is approximately 25 to 30 kcal/mol.[17]

It is seen in a comparison of the data in Tables 3 and 5 and in Table SI-3 in the Supporting Information that the atomic charges on some atoms in the 2-pyrimidinethiols change significantly as the 2-pyrimidinethiol goes from the ground state to the transition state (**TS1**). In general the partial negative charge on N1 decreases, except from APT, the partial positive charge on C2 decreases from CHELPG and MKS, the partial negative charge on N3 decreases from CHELPG and MKS, the partial positive charge on C4 increases from the four methods, the negative charge at C5 increases from the four methods, the partial negative charge on S7 increases from CHELPG and MKS, the partial positive charge on C4 increases from the four methods, and the partial positive charge on the sulfanyl hydrogen increases from the four methods.

Lower energy pathways (relative to **TS1**) via dimers and dimer transition states are available for the tautomerization of

**SCHEME 1**

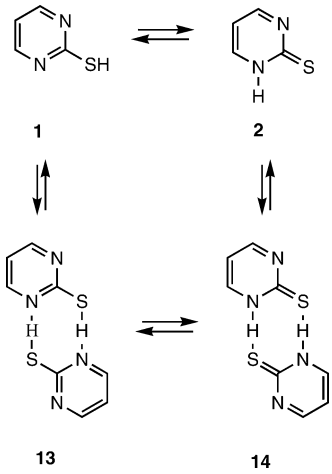


2-pyrimidinethiols in the gas phase.[16] The pyrimidinethiols can exist as homodimers (self-association) and thiol/thione heterodimers in the gas phase and in solution. The dimers of 2-pyrimidinethiol (**13**, **14**, **15**, **TS2**) and 5-methyl-2-pyrimidinethiol (**16**, **17**, **18**, **TS3**) are shown in Figures 7, 8, and 9. The relative energies of the three isomeric dimers (**13**, **14**, **15**) are very sensitive to the level of theory used. B3LYP, B3P86, and B3PW91 with the 6-31+G(d,p) or 6-311+G(d,p) basis set predict the thione dimer (**14**) to be lower in energy than the heterodimer (**15**) which is lower in energy than the thiol dimer (**13**). That is, the relative stability order is **14** > **15** > **13**. CBS-4M predicts the order to be **13** > **15** > **14**. CBS-4M predicts the thiol dimer (**13**) to be 5.52 kcal/mol lower in energy than the thione dimer (**14**) and 4.12 kcal/mol lower in energy than the heterodimer (**15**). For the dimers of 5-methyl-2-pyrimidinethiol (**16**, **17**, **18**) CBS-4M predicts the thiol dimer (**16**) to be 5.76 kcal/mol lower in energy than the thione dimer (**17**) and 4.26 kcal/mol lower in energy than the heterodimer (**18**). Attempts to locate transition states **TS2** and **TS3** with the CBS methods were unsuccessful. Intrinsic reaction coordinate (IRC) calculations show that transition state **TS2** connects thiol dimer (**13**) and thione dimer (**14**) and that transition state **TS3** connects thiol dimer (**16**) and thione dimer (**17**).[16] MP2/6-31+G(d,p)//B3PW91/6-31+G(d,p) predicts transition state **TS2** to be 11.1 kcal/mol higher in energy than thiol dimer (**13**) and **TS3** to be 8.59 kcal/mol higher in energy than thiol dimer (**16**). Although these values for the monomer−dimer promoted tautomerization of (**1**) and (**5**) are qualitative, they are significantly smaller than the respective barriers to tautomerization via the four center transition states **TS1H** and **TS1Me5** (Figure 6, Table 4).[15,16,73−75]

The differences in the B3PW91/6-31+G(d,p) CHELPG partial atomic charges on the atoms in the monomers (Table 3) and in the dimers (Figure 7) are also of interest. For monomer (**1**) and the 2-pyrimidinethiol dimer (**13**), the charge on the S−H hydrogen remains the same and the S7 atom in the dimer (**13**) is 0.02 unit more negative than the one in the monomer (**1**). N1 and N3 of the thiol dimer (**13**) are slightly more positive than those in the monomer (**1**). The sulfur atom in the thione dimer (**14**) is 0.04 unit more negative than the sulfur in the thione monomer (**2**). The charge on the N1−H hydrogen in the 2-pyrimidinethione dimer (**14**) is +0.116 compared to +0.256 in the monomer (**2**), which is a significant change. The charge on N3 remains about the same, but N1 of the dimer (**14**) is more positive than the thione monomer (**2**) by 0.24 unit. In the heterodimer (**15**), the S7−H hydrogen (+0.199) is less positive than the thiol (+0.208) and the N1−H hydrogen is now negative (−0.062) as compared to the thione (**2**, +0.256). The sulfur

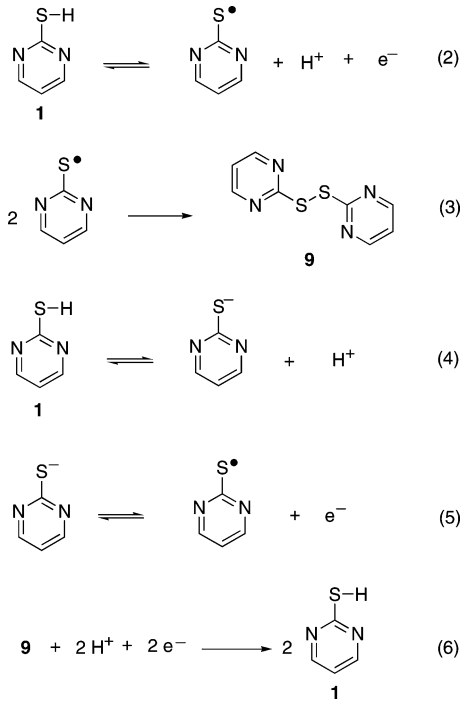


**Figure 10.** Equations depicting the electrochemical oxidation of 2-pyrimidinethiol (**1**).

**SCHEME 2**

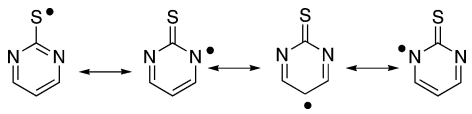

atoms in the heterodimer (**15**) are less negative than the sulfur atoms in the thiol (**1**) and thione (**2**) monomers. The N1 nitrogen atoms in the heterodimer (**15**) are significantly less negative than the N1 atoms in the thiol (**1**) and thione (**2**) monomers.

### Mechanisms of Disulfide Formation During Electrochemical Oxidation

2-Pyridinethiols and 2-pyrimidinethiols (**1** ⇆ **2**; **3** ⇆ **4**; **5** ⇆ **6**; **7** ⇆ **8**) exist in solution with their respective thione tautomers although it is generally accepted that pyridinethiols and pyrimidinethiols exist as thiones rather than thiols in solution.[9,73−76] However, in solution the more reactive sulfanyl group can be oxidized to the corresponding disulfide and the disulfide can be reduced back to the thiol. The complex equilibria among pyrimidinethiols, pyrimidinethiones, and disulfides in solution include dimer formation, reverse thione−disulfide transformation, monomer−dimer equilibrium, thiol/thione equilibrium, and thiol−disulfide interactions (Scheme 1, Figures 7, 8, 9). These equilibria are influenced by concentration, solvent, structure, substituent, and temperature. In aqueous solution the 2-pyrimidinethione tautomers (**1** ⇆ **2**) may be associated with one, two, three, or more water molecules.[16]

The 2-pyrimidinethiols (**1**, p$K_a$ = 7.24; **3**, p$K_a$ = 7.73; **7**, p$K_a$ = 8.54) are weak acids.[8,9,73,77−79] Some of the reactions and processes occurring during the electrochemical oxidation of the sulfanyl group are shown in Scheme 1 and Figure 10. The sulfenyl radical formed in eq 2 can dimerize to the disulfide (**9**, eq 3). Dissociation of the thiol (**1**) affords the 2-thiopyrimidinyl anion (eq 4) that can lose an electron (electron transfer) to form the 2-thiopyrimidinyl radical (eq 5). Equation 6 shows the reduction of the disulfide (**9**) back to 2-pyrimidinethiol (**1**)

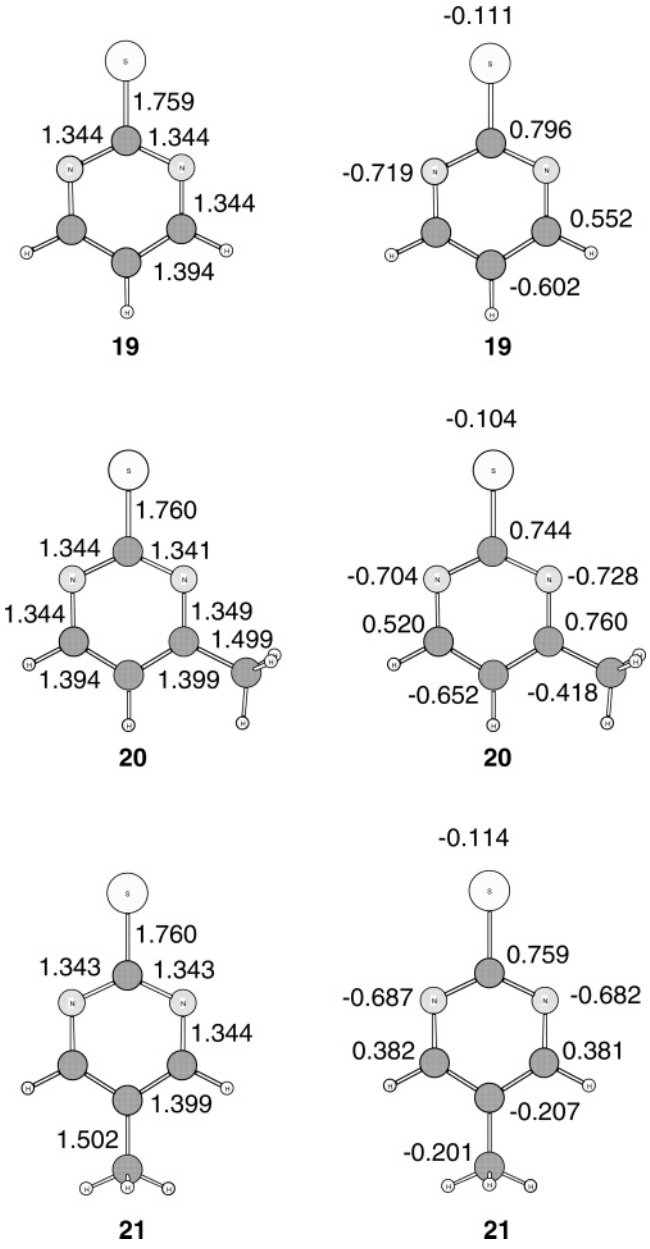


**Figure 11.** UMP2/6-31+G(d,p) optimized structures and CHELPG partial atomic charges for 2-pyrimidinylsulfenyl radicals.

**TABLE 6: Relative Energies for 2-Pyrimidinethiols (1, 3a, 5, 7) and Their Respective 2-Thiopyrimidinyl Radicals (19, 20, 21, 22)[a]**

| level | 19 | 20 | 21 | 22 |
|---|---|---|---|---|
| CBS-QB3 | 89.21 | | | |
| CBS-Q | 89.22 | 88.99 | 89.20 | 89.18 |
| CBS-4M | 89.65 | 88.03 | 89.66 | 89.48 |
| UB3LYP[b] | 90.52 | 90.41 | | 90.23 |
| UB3PW91[b] | 90.44 | 90.34 | | 90.16 |
| UMPW1PW91[b] | 89.90 | 89.82 | 89.88 | 89.64 |
| UMP2[b] | 87.03 | 87.01 | 87.04 | 87.11 |

[a] $E_{rel}$ = $E$(radical + H•) − $E$(thiol). [b] 6-31+G(d,p) basis set.

during the reverse cathodic scan. It is known that sulfenyl radicals can be generated over a wide range of pH.[8,79] Examples include phenylsulfenyl (phenylthiyl) radicals that can be prepared in acidic solutions by abstraction of the sulfanyl hydrogen atom from thiophenols[80] and at pH 11−13.5 by oxidizing thiophenolate anions with azide radicals.[81]

**TABLE 7: Comparison of Experimental and B3PW91/6-31+G(d,p) Calculated Geometric Parameters for Bis(2-pyrimidinyl) Disulfides (9, 10, 11, 12)**

| | **9** | | | **10** | **11** | **12** | |
|---|---|---|---|---|---|---|---|
| parameter | calcd | X-ray[a] | X-ray[b] | calcd | calcd | calcd | X-ray[c] |
| bond length | | | | | | | |
| N1−C2 | 1.328 | 1.348 | 1.337 | 1.336 | 1.326 | 1.325 | 1.324 |
| N1−C6 | 1.336 | 1.337 | 1.332 | 1.333 | 1.336 | 1.342 | 1.347 |
| C2−N3 | 1.336 | 1.326 | 1.318 | 1.325 | 1.336 | 1.333 | 1.327 |
| C2−S7 | 1.785 | 1.782 | 1.781 | 1.787 | 1.786 | 1.788 | 1.782 |
| S7−S7′ | 2.048 | 2.017 | 2.016 | 2.048 | 2.047 | 2.049 | 2.017 |
| S7′−C2′ | 1.785 | 1.786 | | 1.787 | 1.786 | 1.788 | 1.783 |
| N3−C4 | 1.333 | 1.326 | 1.342 | 1.342 | 1.331 | 1.339 | 1.344 |
| C4−H4 (Me) | 1.088 | 0.95 | | 1.499 | 1.090 | 1.500 | 1.491 |
| C4−C5 | 1.394 | 1.385 | 1.370 | 1.398 | 1.400 | 1.398 | 1.376 |
| C5−H5(Me) | 1.064 | 0.96 | | 1.085 | 1.501 | 1.085 | |
| C5−C6 | 1.392 | 1.371 | 1.365 | 1.392 | 1.396 | 1.396 | 1.372 |
| C6−H6 (Me) | 1.089 | 0.92 | | 1.089 | 1.090 | 1.499 | 1.501 |
| bond angle | | | | | | | |
| N1−C2−N3 | 127.6 | 128.2 | 128.1 | 127.8 | 127.1 | 128.0 | 129.0 |
| N1−C2−S7 | 120.8 | 121.5 | 110.6 | 111.4 | 112.2 | 120.7 | 120.8 |
| N1−C6−C5 | 122.6 | 122.9 | 122.1 | 122.6 | 123.6 | 121.0 | 121.5 |
| C2−N1−C6 | 115.6 | 114.3 | 115.4 | 115.1 | 115.6 | 116.0 | 114.6 |
| C2−N3−C4 | 115.7 | 114.7 | 114.5 | 116.7 | 115.8 | 116.2 | 115.2 |
| C2−S7−S7′ | 104.6 | 105.2 | 104.8 | 104.7 | 104.7 | 104.8 | 105.2 |
| C2′−S7′−S7 | 104.6 | 105.2 | | 104.7 | 104.7 | 104.8 | 105.8 |
| N3−C2−S7 | 111.6 | 110.2 | 121.4 | 120.8 | 111.7 | 111.3 | 110.2 |
| N3−C4−C5 | 122.4 | 123.8 | 122.8 | 120.8 | 123.3 | 120.8 | 120.8 |
| C4−C5−C6 | 116.2 | 116.1 | 117.2 | 117.1 | 114.5 | 118.0 | 118.9 |
| torsion angle | | | | | | | |
| N1−C2−S7−S7′ | −6.5 | 2.53 | −174.1 | −174.5 | 7.1 | 5.6 | 178.2 |
| N3′−C2′−S7′−S7 | 174.2 | 0.29 | −178.3 | 6.1 | −173.7 | −174.9 | −0.7 |
| C2−S7−S7′−C2′ | 82.0 | 83.9 | −82.5 | −83.2 | −83.2 | −83.0 | 94.9 |

[a] Reference 24d. [b] References 24a, 24b, bis(2-pyrimidinyl) disulfide dihydrate. [c] Reference 27.

The corresponding sulfenyl radicals (2-pyrimidinyl, **19**; 4-methyl-2-pyrimidinyl, **20**; 5-methyl-2-pyrimidinyl, **21**) from the 2-pyrimidinethiols (**1**), (**3**), and (**5**) were explored. UB3LYP/6-31+G(d,p) and UB3PW91/6-31+G(d,p) did not locate the 5-methyl-2-pyrimidinyl sulfenyl radical (**21**). Figures 5 and 11 show the differences in C−S and C═S bond lengths in the thiols, thiones, and sulfenyl radicals. It is seen that the carbon sulfur bond in the radicals is shorter than the C−S bond in the thiols and longer than the C═S bond in the thiones. Since there are only small changes in the bond angles and bond lengths, the structure of the sulfenyl radical is very similar to that of the corresponding 2-pyrimidenethiol. For example, the C2−S7 bond lengths in the thiols are near 1.765 Å, and in the sulfenyl radicals they are near 1.760 Å. Thus, a significant portion of the single bond character of the C2−S7 bond is maintained in going from the thiol to the sulfenyl radical. The positions of the inductive electron releasing methyl groups ($\sigma_m = -0.07$, $\sigma_p = -0.17$) do not significantly alter the carbon sulfur bond lengths. The sulfanyl group ($\sigma_m = 0.25$, $\sigma_p = 0.15$) and the 2-pyrimidinyl group ($\sigma_I = 0.23$, $\sigma_p = 0.53$) are electron attracting substituents.[84]

The sulfur atom in the sulfenyl radical is electron deficient and shares its unpaired electron with the ring via overlap of the 2p orbitals of carbon and the 3p orbitals of sulfur. The resonance structures in Scheme 2 symbolize the delocalization (sharing) of the unpaired electron. The small electron delocalization of the unpaired electron in the 2-thiopyrimidinyl radicals is similar to that observed for the thiophenoxy radical and the 2-thiopyridyl radical. Additional evidence of the small delocalization is seen in a comparison of the MP2/6-31+G(d,p) computed geometrical parameters for the 2-pyrimidinethiols (Figure 5) and the respective sulfenyl radicals (Figure 11). Table 3, Tables SI-1, SI-2, and SI-3 in the Supporting Information, and Figure 11 give partial atomic charges for 2-pyrimidinethiols (**1**), (**3**), and (**5**) and the corresponding 2-pyrimidinyl (**19**), 4-methyl-2-pyrimidinyl (**20**), and 5-methyl-2-pyrimidinyl (**21**) sulfenyl radicals. It is seen in tables that only the NBO and the Mulliken schemes predict partial positive charges on the sulfur atoms in the three radicals (**19**), (**20**), and (**21**). Unlike the 2-pyrimidinethiols (**1**, **3**, **5**), the predicted charges on the two nitrogen atoms in each sulfenyl radical are equal. The partial atomic charges on N1 and N3 in the sulfenyl radicals are about 0.1 unit more positive than those in the 2-pyrimidinethiols: −0.72 versus −0.84 (CHELPG) and −0.69 versus −0.79 (MKS, Scheme 2).

The CBS-QB3 predicted energy difference [$E_{rel} = E$(radical) + $E$(H•) − $E$(thiol)] between the 2-pyrimidinyl radical and 2-pyrimidinethiol is 89.21 kcal/mol. It is seen in Table 6 that the value of $E_{rel}$ is not very sensitive to the presence of the methyl groups on the heteroaromatic ring. It is also seen in Table 6 that CBS-QB3, CBS-Q, and CBS-4M predict similar values of $E_{rel}$ for the four 2-pyrimidinethiols (**1**, **3a**, **5**, **7**) and their respective sulfenyl radicals (**19**, **20**, **21**, **22**) while the hybrid density functionals predict similar but slightly larger values.

### Structures of Disulfides

B3PW91/6-31+G(d,p) predicts bis(4-methyl-2-pyrimidinyl) disulfide (**10**) to be 8.31 kcal/mol lower in energy than bis(5-methyl-2-pyrimidinyl) disulfide (**11**). In disulfide steric arguments predict that the preferred conformation should have a C−S−S−C dihedral angle of 180°. However, owing in part to orbital interactions and to interatomic repulsive interactions between sulfur lone pairs, the conformational preferences of many disulfides have C−S−S−C torsion angles around 90° with the disulfide linkage being approximately gauche. In the gauche conformation the disulfides possess chirality that leads to enantiomers or disastereomers. Although the crystal structures of many organic disulfides are known, structures of heteroaromatic disulfides are less common. The crystal structures of bis-

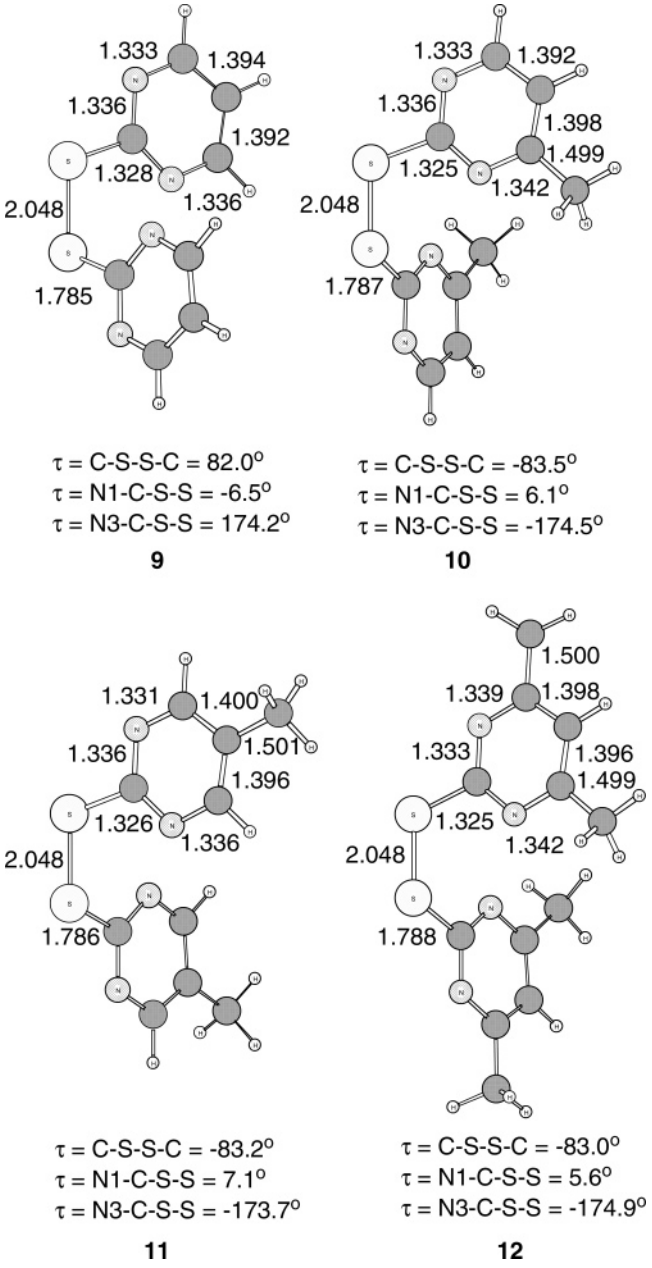


**Figure 12.** B3PW91/6-31+G(d,p) optimized structures for bis(2-pyrimidinyl) disulfides (**9**), (**10**), (**11**), and (**12**).

(2-pyrimidinyl) disulfide (**9**),[24] bis(2-pyrimidinyl) disulfide dihydrate,[24] and bis(4,6-dimethyl-2-pyrimidinyl) disulfide (**12**)[27] have been reported. The B3PW91/6-31+G(d,p) calculated geometrical parameters for disulfides (**9**) and (**12**) are in excellent agreement with their X-ray crystal data (Table 7). The calculated and the experimental C−S−S bond angles in the disulfides are near 105°. B3PW91/6-31+G(d,p) predicts the C−S−S−C torsion angles in disulfides (**9**), (**10**), (**11**), and (**12**) to be 82.0°, −83.2°, −83.2°, and −83.0°, respectively, (Figure 12). The X-ray values[24a,24b] for the C−S−S−C torsion angle in disulfide (**9**) and its dihydrate are 83.9° and 82.5°, and for disulfide (**12**) it is 94.9°.[27]

The crystal structure of bis(2-pyrimidinyl) disulfide dihydrate is unusual for a disulfide owing to the presence of water molecules, and it has an eclipsed conformation with the pyrimidinyl rings. Bis(2-pyrimidinyl) disulfide (**9**) crystallizes to a structure with two crystallographically nonequivalent molecules. The four pyrimidine rings are planar and have similar bond angles and bond lengths. There are several contacts in the crystal structure between ring nitrogen lone pairs and ring hydrogens. The packing of the molecules in the crystal of 2-pyridinethiol has two molecules linked to each other by two bent N−H−S hydrogen bonds through a crystallographic center of symmetry. The calculated N−C−S−S torsion angles (175° and 6°) in disulfides (**9**), (**10**), (**11**), and (**12**) are very similar. The pyrimidine rings in the solid disulfide (**12**) are almost perpendicular with a dihedral angle of 96.9°. The N−C−S−S torsion angles in the crystal structure of disulfide (**12**) are 178.2° and −0.7°, showing that the sulfur atoms and the pyrimidine rings to which they are attached are coplanar.[27]

The calculated and experimental C−S bond lengths of the disulfides (**9**, **10**, **11**, **12**) are near 1.786 Å and are close to the values found in the 2-pyrimidinethiols (**1**, **3**, **5**, **7**, Figure 5), 2-pyridyl disulfide (1.785 Å),[82] diphenyl disulfide (1.788 Å),[83] and other organic disulfides. These C−S bond lengths in the disulfides are longer than the predicted C═S bonds in the 2-pyrimidinethiones (**2**, **4**, **6**, **8**) and 2-pyridinethione (1.698 Å).[82] This suggests that there is little or no $\pi$ electron delocalization between the ring and the disulfide group. The S−S bond length in each of the disulfides (**9**), (**10**), (**11**), and (**12**) is 2.048 Å, which is close to the value in the crystal structure and longer than that in crystalline 2-pyridine disulfide (2.016 Å) and in solid diphenyl disufide (2.023 Å).

## Conclusions

The methods and basis sets used in this study predicted consistent and accurate electronic energies and structures for a wide range of compounds with important sulfur containing functional groups including thiols, thiones, disulfides, sulfenyl radicals, thiol dimers, thione dimers, and transition states at reasonable computational costs. The less polar 2-pyrimidinethiol is lower in energy than its 2-pyrimidinethione tautomer in the gas phase. CBS-QB3, CBS-Q, CCD, CCSD, QCISD, and MP2, predict similar values for the energy difference ($E_{rel}$) between respective tautomers. The hybrid density functionals (B3LYP, B3P86, B3PW91, MPW1PW91) predict smaller values for $E_{rel}$ between tautomers than any of the other models used in this study. Increasing the number of methyl groups at positions 4 and 6 on the 2-pyrimidinethiol ring lowers the energy difference ($E_{rel}$) between tautomers. CBS-4M predicts the 2-pyrimidinethiol dimer (1**3**) to be 5.52 and 4.12 kcal/mol, respectively, lower in energy than the isomeric thione dimer (**14**) and heterodimer (**15**). The intramolecular four center transition states (**TS1**) for the tautomerization of 2-pyrimidinethiols (**1**, **3**a, **3b**, **5**, **7**) in the gas phase have higher activation barriers than the pathways involving dimers and dimer transition states. The anodic oxidation of the 2-pyrimidinethiols at an applied potential under a dinitrogen atmosphere gave only disulfides that were easily separated and purified. Dimers, dimer transition states, and sulfenyl radicals are also involved in the electrochemical oxidation of the 2-pyrimidinethiols. Small electron delocalization (resonance) is observed in the sulfenyl radicals. Among the five schemes explored for predicting partial atomic charges, the Mulliken computed charges deviate the most from the other four schemes and CHELPG and MKS computed the most consistent charges irrespective of the level of theory used in this study.

**Supporting Information Available:** Experimental details and spectral data for the disulfides and tables of partial atomic charges. This information is available free of charge via the Internet at http://pubs.acs.org.

## References and Notes


(1) (a) *S-centered Radicals*; Alfassi, Z. B., Ed.; Wiley: Chichester, U.K., 1999. (b) *Sulfur-Centered Reactive Intermediates in Chemistry and Biology*; Chatgilialoglu, C., Asmus, K.-D., Eds.; NATO ASI Series; Plenum Press: New York, 1990. (c) Gonzalez, V. M.; Fuertes, M. A.; Perez-Alvarez, M. J.; Cervantes, G.; Moreno, V.; Alonso, C.; Perez, J. M. *Biochem. Pharm.* **2000**, *60*, 371−379. (d) Toda, F.; Tanaka, K.; Sato, J. *Tetrahedron: Asymmetry* **1993**, **4**, 1771−1774.

(2) Freeman, F.; Keindl, M. C. *Sulfur Rep.* **1985**, *4*, 231−305.

(3) (a) Pinheiro, L. S.; Temperini, M. L. A. *Surf. Sci.* **1999**, *441*, 45−52. (b) Pinheiro, L. S.; Temperini, M. L. A. *Surf. Sci.* **1999**, *441*, 53−64. (c) Pinheiro, L. S.; Temperini, M. L. A. *Appl. Surf. Sci.* **2001**, *171*, 89−100. (d) Davis, J. J.; Hill, H. A. O.; Yamada, R.; Naohara, H.; Uosaki, K. *J. Chem. Soc., Faraday Trans.* **1988**, *94*, 1315−1319. (e) Pang, Y. S.; Hwang, H. J.; Kim, M. S. *J. Mol. Struct.* **1998**, *441*, 63−76.

(4) (a) Huber, F.; Schmiedgen, R.; Schurmann, M.; Barbieri, R.; Ruisi, G.; Silvestri, A. *Appl. Organomet. Chem.* **1997**, *11*, 869−888. (b) Schmiedgen, R.; Huber, F.; Schurmann, M.; Silvestri, A.; Ruisi, G.; Rossi, M.; Barbieri, R. *Appl. Organomet. Chem.* **1998**, *12*, 861−871.

(5) (a) Contretras, J. G.; Seguel, G. V.; Alderete, J. B. *Spectrochim. Acta* **1994**, *50A*, 371−374. (b) Contretras, J. G.; Alderete, J. B. *Bol. Soc. Chil. Quim.* **1994**, *39*, 17−21. (c) Contretras, J. G.; Alderete, J. B. *Folia Chim. Theor. Lat.* **1991**, *19*, 211−223.

(6) (a) Zhang, H.-L.; Evans, S. D.; Henderson, J. R.; Miles, R. L.; Shen, T. *J. Phys. Chem. B* **2003**, *107*, 6087−6095. (b) Zhang, H.-L.; Chen, M.; Li, H.-L. *J. Phys. Chem. B* **2000**, *104*, 28−36.

(7) (a) Calvente, R. M.; Campos-Martin, J. M.; Fierro, J. L. G. *Catal. Commun.* **2002**, *3*, 247−251. (b) Taqui Khan, M. M.; Chatterjee, D.; Hussain, A.; Moiz, A. *Polyhedron* **1990**, *22*, 2681−2687. (c) Fernandez-Gala, R.; Manzano, B. R.; Otero, A.; Poujaud, N.; Kubicki, M. *J. Organomet. Chem.* **1999**, *579*, 321−327. (d) Romero, J.; Duran, M. L.; Rodriguez, A.; Garcia-Vazquez. J. A.; Sousa, A.; Rose, D. J.; Zubieta, J. *Inorg. Chim. Acta* **1998**, *274*, 131−136.

(8) Tripathi, G. N. R.; Clements, M. *J. Phys. Chem. B* **2003**, *107*, 11125−11132.

(9) (a) Stoyanov, S.; Stoyanova, T.; Antonov, L.; Karagiannidis, P.; Akrivos, P. *Monatsh. Chem.* **1996**, *127*, 495−504 and references therein. (b) Stoyanov, S.; Petkov, I.; Antonov, L.; Stoyanova, T.; Karagiannidis, P.; Aslanidis, P. *Can. J. Chem.* **1990**, *68*, 1482−1489. (c) Stoyanov, S.; Stoyanova, T.; Arkivos, P. D.; Karagiannidis, P.; Nikolov, P. *J. Heterocycl. Chem.* **1996**, *33*, 927−931.

(10) (a) Brown, D. J.; Hoskins, J. A. *J. Chem. Soc., Perkin Trans. 1* **1972**, 522−527. (b) von Angerer, S. *Sci. Synth.* **2004**, *16*, 379−572. (c) Skoetsch, C.; Haffmanns, G.; Breitmaier, Eberhard *Chem. Ber.* **1977**, *110*, 2872−2879. (d) Rylski, L.; Sorm, F.; Arnold, Z. *Collect. Czech. Chem. Commun.* **1959**, *24*, 1667−1671.

(11) (a) Martos-Calvente, R.; O'Shea, V. A.; de la Peña; Campos-Martin, J. M.; Fierro, J. L. G. *J. Phys. Chem. A* **2003**, *107*, 7490−7495. (b) Martos-Calvente, R.; Campos-Martin, J. M.; Fierro, J. L. G. *Catal. Commun.* **2002**, *3*, 247−251. (c) Lang, E. S.; Oliveira, G. M. de; Casagrande, G. A.; Vásquez-Lopez, E. M. *Inorg. Chem. Commun.* **2003**, *6*, 1297−1301. (d) Cai, C.-X. *J. Electroanal. Chem.* **1995**, *393*, 119−122. (e) Hong, F.-E.; Huang, Y.-L.; Chen, P.-P; Chang, Y.-C. *J. Organomet. Chem.* **2002**, *655*, 49−54. (f) Khan, M. M. T.; Chatterjee, D.; Hussain, A.; Moiz, M. A. *Polyhedron* **1990**, *9*, 2681−2687.

(12) Berndt, M.; Kwiatowski, J. S.; Budzinski, J.; Szczodrowska, B. *Chem. Phys. Lett.* **1973**, *19*, 246−250.

(13) Contreras, J. G.; Alderete, J. B. *J. Mol. Struct. (THEOCHEM)* **1991**, *231*, 257−265.

(14) Nowak, M. J.; Rostkowska, H.; Lapinski, L.; Leszczynski, J.; Kwiatkowski, J. S. *Spectrochim. Acta* **1991**, *47A*, 339−353.

(15) Lima, M. C. P.; Coutinho, K.; Canuto, S.; Rocha, W. R. *J. Phys. Chem. A* **2006**, *110*, 7253−7261.

(16) Freeman, F.; Po, H. N. *J. Phys. Chem. A* **2006**, *110*, 7904−7912.

(17) Moran, D.; Sukcharoenphon, K.; Puchta, R.; Schaefer, H. F., III; Schleyer, P. V. R.; Hoff, C. D. *J. Org. Chem.* **2002**, *67*, 9061−9069 and references cited therein.

(18) (a) Xantheas, S.; Dunning, T. H., Jr. *J. Phys. Chem.* **1993**, *97*, 6616. (b) Smart, B. A.; Schiesser, C. H. *J. Comput. Chem.* **1995**, *16*, 1055. (c) Ruttink, P. J. A.; Burgers, P. C.; Francis, J. T.; Terlouw, J. K. *J. Phys. Chem.* **1996**, *100*, 9694. (d) Frank, A. J.; Sadilek, M.; Ferrier, J. G.; Turecek, F. *J. Am. Chem. Soc.* **1997**, *118*, 11321. (e) Frank, A. J.; Sadilek, M.; Ferrier, J. G.; Turecek, F. *J. Am. Chem. Soc.* **1997**, *119*, 12343. (f) Turecek, F. *J. Phys. Chem. A* **1998**, *102*, 4703.

(19) Freeman, F.; Cha, C. *J. Phys. Org. Chem.* **2004**, *17*, 32−41.

(20) Freeman, F.; Cha, C. *Int. J. Quantum Chem.* **2004**, *96*, 443−455.

(21) Freeman, F.; Bathala, R. M.; Huang, A. C.; Jackson, T. K.; Lopez-Mercado, A. Z.; Phung, S.; Suh, J.; Valenica, Jr., D. O. *Int. J. Quantum Chem.* **2006**, *106*, 2390−2397.

(22) Tsuzuki, S.; Lüthi, H. P. *J. Chem. Phys.* **2001**, *114*, 3949−3957.

(23) (a) Kwiatkowski, J. S.; Leszczynski, J. *J. Mol. Struct.* **1996**, *376*, 325−342. (b) Nowak, M. J.; Lapinski, L.; Rostkowska, H.; Les, A.; Adamowicz, L. *J. Chem. Phys.* **1990**, *94*, 7406. (c) Armstrong, D. R.; Davies, J. E. D.; Feeder, N.; Lamb, E.; Longridge, J. L.; Rawson, J. M.; Snaith, R.; Wheatley, A. E. H. *J. Mol. Model.* **2000**, *6*, 234.

(24) (a) Jensen, G. B.; Smith, G.; Sagatys, D. S.; Healy, P. C.; White, J. M. *Acta Crystallogr., Sect. E: Struct. Rep. Online* **2004**, *E60*, o2438−o2440. (b) Furberg, S.; Solbakk, J. *Acta Chem. Scand.* **1973**, *27*, 2536−2542. (c) Boyd, D. B.; Lipkowitz, K. B. *J. Comput. Chem.* **1981**, *2*, 324−333. (d) Simmons, C. J.; Lundeen, M.; Seff, K. *Inorg. Chem.* **1979**, *18*, 3444−3452.

(25) Hurst, D. T.; Jonas, S. G.; Outram, J.; Patterson, R. A. *J. Chem. Soc., Perkin Trans. 1* **1977**, 1688−1692.

(26) Mahieu, J.-P.; Gosselet, M.; Sebille, B.; Beuzard, Y. *Synth. Commun.* **1986**, *16*, 1709−1722.

(27) (a) Castro, J. A.; Romero, J.; Garcia-Vazquez, J. A.; Castiñeiras, A.; Sousa, A.; Zubieta, J. *Polyhedron* **1995**, *14*, 2841−2847. (b) Alcock, N. W.; Pennington, M. *Acta Crystallogr.* **1990**, *C46*, 18−21.

(28) (a) Olby, B. G.; Robinson, S. D. *Inorg. Chim. Acta* **1989**, *165*, 153−162. (b) Au, Y.-K.; Cheung, K.-K.; Wong, W.-T. *J. Chem. Soc., Dalton Trans.* **1995**, 1047−1057.

(29) Ji, C.; Ahmida, M.; Chahma, M.; Houmam, A. *J. Am. Chem. Soc.* **2006**, *128*, 15423−15431.

(30) (a) Kong, J.; White, C. A.; Krylov, A. I.; Sherrill, C. D.; Adamson, R. D.; Furlani, T. R.; Lee, M. S.; Lee, A. M.; Gwaltney, S. R.; Adams, T. R.; Ochsenfeld, C.; Gilbert, A. T. B.; Kedziora, G. S.; Rassolov, V. A.; Maurice, D. R.; Nair, N.; Shao, Y.; Besley, N. A.; Maslen, P. E.; Domboski, J. P.; Daschel, H.; Zhang, W.; Korambath, P. P.; Baker, J.; Byrd, E. F. C.; Voorhis, T. V.; Oumi, M.; Hirata, S.; Hsu, C.-P.; Ishikawa, N.; Florian, J.; Warshel, A.; Johnson, B. G.; Gill, P. M. W.; Head-Gordon, M.; Pople, J. A. *J. Comput. Chem.* **2000**, *21*, 1532−1548. (b) The Spartan '04 Macintosh and Spartan '02 Unix programs are available from Wavefunction, Inc., Irvine, CA 92612.

(31) Frisch, M. J.; Trucks, G. W.; Schlegel, H. B.; Scuseria, G. E.; Robb, M. A.; Cheeseman, J. R.; Montgomery, J. A., Jr.; Vreven, T.; Kudin, K. N.; Burant, J. C.; Millam, J. M.; Iyengar, S. S.; Tomasi, J.; Barone, V.; Mennucci, B.; Cossi, M.; Scalmani, G.; Rega, N.; Petersson, G. A.; Nakatsuji, H.; Hada, M.; Ehara, M.; Toyota, K.; Fukuda, R.; Hasegawa, J.; Ishida, M.; Nakajima, T.; Honda, Y.; Kitao, O.; Nakai, H.; Klene, M.; Li, X.; Knox, J. E.; Hratchian, H. P.; Cross, J. B.; Adamo, C.; Jaramillo, J.; Gomperts, R.; Stratmann, R. E.; Yazyev, O.; Austin, A. J.; Cammi, R.; Pomelli, C.; Ochterski, J. W.; Ayala, P. Y.; Morokuma, K.; Voth, G. A.; Salvador, P.; Dannenberg, J. J.; Zakrzewski, V. G.; Dapprich, S.; Daniels, A. D.; Strain, M. C.; Farkas, O.; Malick, D. K.; Rabuck, A. D.; Raghavachari, K.; Foresman, J. B.; Ortiz, J. V.; Cui, Q.; Baboul, A. G.; Clifford, S.; Cioslowski, J.; Stefanov, B. B.; Liu, G.; Liashenko, A.; Piskorz, P.; Komaromi, I.; Martin, R. L.; Fox, D. J.; Keith, T.; Al-Laham, M. A.; Peng, C. Y.; Nanayakkara, A.; Challacombe, M.; Gill, P. M. W.; Johnson, B.; Chen, W.; Wong, M. W.; Gonzalez, C.; and Pople, J. A. *Gaussian 03*, revision A.1; Gaussian, Inc.: Pittsburgh, PA, 2003.

(32) Foresman, J. B.; Frisch, A. *Exploring Chemistry with Electronic Structure Methods*, 2nd ed.; Gaussian, Inc.: Pittsburgh, PA, 1996.

(33) (a) Becke, A. D. *Phys. Rev.* **1988**, *A38*, 3098−3100. (b) Lee, C.; Yang, W.; Parr, R. G. *Phys. Rev.* **1988**, *B37*, 785−789. (c) Vosko, S. H; Wilk, L.; Nusair, M. *Can. J. Phys.* **1980**, *58*, 1200−1211.

(34) Becke, A. D. *J. Chem. Phys.* **1993**, *98*, 5648.

(35) Stephens, P. J.; Devlin, F. J.; Chabalowski, C. F.; Frisch, M. J. *J. Phys. Chem.* **1994**, *98*, 11623−11627.

(36) (a) Harris, J.; Jones, R. O. *J. Phys. Chem.* 1**974**, *F4*, 1170. (b) Gunnarson, O.; Lundqvist, B. I. *Phys. Rev. B* **1976**, *13*, 4274. (c) Harris, J. *J. Phys. Rev. A* **1948**, *29*, 1648.

(37) Perdew, J. P. *Phys. Rev. B* **1986**, *33*, 8822.

(38) Perdew, J. P.; Burke, K.; Wang, Y. *Phys. Rev. B* **1996**, *54*, 16533−16539 and reference cited therein.

(39) Adamo, C.; Barone, V. *J. Chem. Phys.* **1998**, *108*, 664.

(40) Hehre, W. J.; Radom, L.; Schleyer, P. v.; Pople, J. A. *Ab Initio Molecular Orbital Theory*; Wiley: New York, 1986.

(41) Krishnan, R.; Binkley, J. S.; Seeger, R.; Pople, J. A. *J. Chem. Phys.* **1980**, *72*, 650.

(42) McLean, A. D.; Chandler, G. S. *J. Chem. Phys.* **1980**, *72*, 5639.

(43) (a) Ditchfield, R.; Hehre, W. J.; Pople, J. A. *J. Chem. Phys.* **1971**, *54*, 724. (b) Gordon, M. S. *Chem. Phys. Lett.* **1980**, *76*, 163.

(44) (a) Francl, M. M.; Pietro, W. J.; Hehre, W. J.; Binkley, J. S.; DeFrees, D. J.; Pople, J. A.; Gordon, M. S. *J. Chem. Phys.* **1982**, *77*, 3654. (b) Rassolov, V. A.; Ratner, M. A.; Pople, J. A.; Redfern, P. C.; Curtiss, L. A. *J. Comput. Chem.* **2001**, *22*, 976.

(45) (a) Dunning, T. H. *J. Chem. Phys.* **1989**, *90*, 1007. (b) Woon, D.; Dunning, T. H. *J. Chem. Phys.* **1993**, *98*, 1358. (c) Woon, D.; Dunning, T. H. *J. Chem. Phys.* **1995**, *103*, 4572. (d) Wilson, A.; van Mourik, T.; Dunning, T. H., Jr. *J. Mol. Struct. (THEOCHEM)* **1997**, *388*, 339.

(46) *CCCBDB Vibrational Frequency Scaling Factors*, http://srdata.nist.gov/cccbdb/vsf.asp.

(47) Lynch, B. J.; Zhao, Y.; Truhlar, D. G. *Database of Frequency Scaling Factors for Electronic Structure Methods*, **2003**, http://comp.chem.umn.edu/database/freq_scale.htm.

(48) Bartlett, R. J.; Purvis, G. D. *Int. J. Quantum Chem*. **1978**, *14*, 516.
(49) Purvis, G. D.; Bartlett, R. J. *J. Chem. Phys*. **1982**, *76*, 1910.
(50) Pople, J. A.; Krishnan, R.; Schlegel, H. B.; Binkley, J. S. *Int. J. Quantum Chem*. **1978**, *14*, 545.
(51) Pople, J. A.; Head-Gordon, M.; Raghavachari, K. *J. Chem. Phys*. **1987**, *87*, 5968.
(52) (a) Gauss, J.; Cremer, C. *Chem. Phys. Lett*. **1988**, *150*, 280. (b) Salter, E. A.; Trucks, G. W.; Bartlett, R. J. *J. Chem. Phys*. **1989**, *90*, 1752.
(53) (a) Nyden, M. R.; Petersson, G. A. *J. Chem. Phys*. **1981**, *75*, 1843. (b) Petersson, G. A.; Al-Laham, M. A. *J. Chem. Phys*. **1991**, *94*, 6081. (c) Petersson, G. A.; Tensfeldt, T.; Montgomery, J. A., Jr. *J. Chem. Phys*. **1991**, *94*, 6091. (d) Montgomery, J. A., Jr.; Ochterski, J. W.; Petersson, G. A. *J. Chem. Phys*. **1994**, *101*, 5900.
(54) (a) Ochterski, J. W.; Petersson, G. A.; Montgomery, J. A., Jr. *J. Chem. Phys*. **1996**, *104*, 2598. (b) Montgomery, J. A., Jr.; Frisch, M. J.; Ochterski, J. W.; Petersson, G. A. *J. Chem. Phys*. **2000**, *112*, 6532−6542.
(55) (a) Curtiss, L. A.; Raghavachari, K.; Trucks, G. W.; Pople, J. A. *J. Chem. Phys*. **1991**, *94*, 7221. (b) Curtiss, L. A.; Raghavachari, K.; Redfern, P. C.; Rassolov, V.; Pople, J. A. *J. Chem. Phys*. **1998**, *109*, 7764−7776.
(56) Curtiss, L. A.; Redfern, P. C.; Raghavachari, K.; Rassolov, V.; Pople, J. A. *J. Chem. Phys*. **1999**, *110*, 4703.
(57) Martin, J. M. L.; Oliveria, G. *J. Chem. Phys*. **1999**, *111*, 1843−1856.
(58) Parthiban, S.; Martin, J. M. L. **2001**, *114*, 6014.
(59) Clark, T.; Chandrasekhar, J.; Spitznagel, G. W.; Schleyer, P. V. R. *J. Comput. Chem*. **1983**, *4*, 294.
(60) (a) Oae, S. *Organic Chemistry Structure and Mechanism*; CRC Press: Boca Raton, FL, 1991. (b) Block, E. Reactions of Organosulfur Compounds. In *Organic Chemistry*; Blomquist, A. T, Wasserman, H. H., Eds.; Academic Press, New York, 1978; Vol. 37.
(61) Katritzky, A. R.; Jug, K.; Oniciu, D. C. *Chem. Rev*. **2001**, *101*, 1421−1449.
(62) Del Bene, J. B. In *The Encyclopedia of Computational Chemistry*; Schleyer, P. v. R., Allinger, N. L., Clark, T., Gasteiger, J., Kollman, P. A., Schaefer, H. F., III, Schreiner, P. R., Eds.; Wiley: Chichester, U.K., 1998; pp 1263−1286.
(63) Wiberg, K. B.; Rablen, P. R. *J. Comput. Chem*. **1993**, *14*, 1504−1518.
(64) Hehre, W. J. *A Guide to Molecular Mechanics and Quantum Chemical Calculations*; Wavefunction, Inc.: Irvine, CA, 2003.
(65) Mulliken, R. S. *J. Phys. Chem*. **1955**, *23*, 1833.
(66) (a) Reed, A. E.; Curtiss, L. A.; Weinhold, F. *Chem. Rev*. **1988**, *88*, 899. (b) Weinhold, F.; Carpenter, J. E. *Plenum* **1988**, 227. (c) Reed, A. E.; Weinhold, F. *J. Chem. Phys*. **1986**, *84*, 2428. (d) Reed, A. E.; Weinstock, R. B.; Weinhold, F. *J. Chem. Phys*. **1985**, *83*, 735.
(67) (a) Breneman, C. M.; Wiberg, K. B. *J. Comput. Chem*. **1990**, *11*, 361. (b) Chirlian, L. E.; Francl, M. M. *J. Comput. Chem*. **1987**, *8*, 894.
(68) (a) Besler, B. H.; Merz, K. M., Jr.; Kollman, P. K. *J. Comput. Chem*. **1990**, *11*, 431. (b) Singh, U. C.; Kollman, P. A. *J. Comput. Chem*. **1984**, *5*, 129.
(69) Cioslowski, J. *J. Am. Chem. Soc*. **1989**, *111*, 8333.
(70) (a) King, W. T.; Mast, G. G.; Blanchette, P. P. *J. Chem. Phys*. **1972**, *56*, 4440. (b) King, W. T.; Mast, G. G. *J. Chem. Phys*. **1976**, *80*, 2521. (c) Person, W. B.; Newton, J. H. *J. Chem. Phys*. **1974**, *61*, 1040. (d) Person, W. B.; Newton, J. H. *J. Chem. Phys*. **1976**, *64*, 3036.
(71) (a) Crews, P.; Rodríguez, J.; Jaspers, M. *Organic Structure Analysis*; Oxford: New York, 1998. (b) Lambert, J. B.; Shurvell, H. F.; Lightner, D. A.; Cooks, R. G. *Organic Structural Spectroscopy*; Prentice-Hall: Upper Saddle River, NJ, 1998. (c) Silverstein, R. M.; Webster, F. X.; Kiemle, D. J. *Spectrometric Identification of Organic Compounds*, 7th ed.; Wiley: New York, 2005. (d) Lautié, A.; Hervieu, J.; Belloc, *J. Spectrochim. Acta* **1983**, *39A*, 367−372. (e) Gupta, S. P.; Sharma, S.; Goel, R. K. *Specrochim. Acta* **1986**, *42A*, 1171−1179.
(72) (a) Schlegel, H. B. *J. Comput. Chem*. **2003**, *24*, 1514−1527. (b) Ayala, P. Y.; Schlegel, H. B. *J. Chem. Phys*. **1997**, *107*, 375−384. (c) Gonzalez, C.; Schlegel, H. B. *J. Chem. Phys*. **1990**, *90*, 2154−2161. (d) Gonzalez, C.; Schlegel, H. B. *J. Phys. Chem*. **1990**, *94*, 5523−5527. (e) Peng, C.; Schlegel, H. B. *Isr. J. Chem*. **1993**, *33*, 449. (f) Peng, C.; Ayala, P. Y.; Schlegel, H. B.; Frisch, M. J. *J. Comput. Chem.* **1995**, *16*, 49.
(73) (a) Beak, P.; Covington, J. B.; Smith, J. G.; White, J. M.; Zeigler, J. M. *J. Org. Chem*. **1980**, *45*, 1354. (b) Beak, P.; Bobham, J.; Lee, J. T. *J. Am. Chem. Soc*. **1968**, *90*, 1569. (c) Beak, P.; Covington, J. B.; Smith, J. G. *J. Am. Chem. Soc*. **1976**, *98*, 8284. (d) Beak, P.; Fry, I. S., Jr.; Steela, F. *J. Am. Chem. Soc.* **1976**, *98*, 171. (e) Beak, P. *Acc. Chem. Res*. **1977**, *10*, 186.
(74) (a) Bensaude, O.; Dreyfus, M.; Dodin, G.; Dubois, J.-E. *J. Am. Chem. Soc*. **1977**, *99*, 4438−4446. (b) Bensaude, O.; Chevrier, M.; Dubois, J.-E. *J. Am. Chem. Soc*. **1978**, *100*, 7055−7060. (c) Bensaude, O.; Chevrier, M.; Dubois, J.-E. *J. Am. Chem. Soc.* **1979**, *101*, 2423−2429. (d) Chevrier, M.; Guillierez, J.; Dubois, J.-E. *J. Chem. Soc., Perkin Trans. 2* **1983**, 979−982.
(75) (a) Field, M. J.; Hillier, I. H. *J. Chem. Soc., Perkin Trans. 2* **1987**, 617−622 and references therein. (b) Parchment, O. G.; Burton, N. A.; Hillier, I. H.; Vincent, M. A. *J. Chem. Soc., Perkin Trans. 2* **1993**, 861−863.
(76) (a) Katritzky, A. R.; Lagowski, J. M. *Adv. Heterocycl. Chem*. **1963**, *1*, 312. (b) Elguero, J.; Marzin, C.; Katrizky, A. R.; Linda, P. The Tautomerism of Heterocycles. In *Adv. Heterocycl. Chem. Supplement 1*; Katritzky, A. R., Boulton, A. J., Eds.; Academic Press: New York, 1976; p 7.
(77) Albert, A.; Barlin, J. *J. Chem. Soc*. **1959**, 2384.
(78) Bosch, E.; Rafols, C.; Roses, M. *Talanta* **1989**, *36*, 1227−1231.
(79) (a) Khin, C.; Shen, S.-C.; Mahmud, R.; Weiss, M.; Po, H. N. *J. Coord. Chem*. **2004**, *57*, 1015−1026. (b) Po, H. N.; Hunting, J. L.; Mahmud, R.; Radzian, R.; Shen, S.-C. *J. Coord. Chem*. **2000**, *51*, 399−416. (c) Trismitro, R.; Po, H. N. *J. Coord. Chem*. **1988**, *17*, 1−14.
(80) Armstrong, D. A.; Sun, Q.; Tripathi, G. N. R.; Schuler, R. H.; McKinnon, D. *J. Phys. Chem*. **1993**, *97*, 5611.
(81) Armstrong, D. A.; Sun, Q.; Schuler, R. H. *J. Phys. Chem*. **1996**, *100*, 9892−9899.
(82) (a) Penfold, B. R. *Acta Crystallogr*. **1953**, *6*, 707−713. (b) Ohms, U.; Guth, H.; Kutoglu, A.; Scheringer, C. *Acta Crystallogr*. **1982**, *B38*, 831−834. (c) Higashi, L. S.; Lundeen, M.; Seff, K. *J. Am. Chem. Soc*. **1978**, *100*, 8101−8106.
(83) (a) Sacerdoti, M.; Gill, G.; Domiano, P. *Acta Crystallogr*. **1975**, *31B*, 327. (b) Raghavan, N. V.; Seff, K. *Acta Crystallogr*. **1977**, *33B*, 386.
(84) Hansch, C.; Leo, A.; Taft, R. W. *Chem. Rev*. **1991**, *91*, 165−195.